THE EFFECTS OF *BIFIDOBACTERIUM LONGUM* NCC3001 ON AH NEURON EXCITABILITY AND SLOW WAVE ACTIVITY OF THE MOUSE INTESTINE

By

AMIR KHOSHDEL, HON.B.Sc.

A Thesis

Submitted to the School of Graduate Studies

in Partial Fulfillment of the Requirements

for the Degree

Master of Science

McMaster University

MASTER OF SCIENCE (2012) MCMASTER UNIVERSITY
(Medical Sciences) Hamilton, Ontario

TITLE: The effects of *Bifidobacterium longum* NCC3001 on AH neuron excitability and slow wave activity of the mouse intestine

AUTHOR: Amir Khoshdel, Hon.B.Sc. (McMaster University)

SUPERVISOR: Professor Jan D. Huizinga (Ph.D.)

NUMBER OF PAGES: xv, 109

ABSTRACT

The small intestine holds an intrinsic ability to digest and absorb nutrients from the food we intake without intervention from the central nervous system. This ability is made possible by the population of cells that inhabit the gut, particularly interstitial cells of Cajal of the myenteric plexus and sensory primary intrinsic neurons (AH cells), which ultimately influence muscle function and motility. The AH cells are the first neurons in the hierarchy of sensory neurons in the gut and are therefore a perfect candidate to test the effects of *Bifidobacterium longum* NCC3001 supernatant since in a physiological setting the metabolites secreted by this bacterium can interact with the AH cells directly or indirectly through absorption by the mucosa.

The probiotic *Bifidobacterium longum* NCC3001 has been shown to normalize anxiety-like behaviour and hippocampal brain derived neurotropic factor (BDNF) levels in mice infected with *Trichuris muris* in a model of infectious colitis. Utilizing a chronic model of colitis, a study was conducted to decipher whether or not the anxiolytic effects of *Bifidobacterium longum* NCC3001 involved the vagus. My specific objective in this study was to find evidence for interaction between *B.longum* NCC3001 and myenteric neurons as a potential route for *B.longum* NCC3001 to influence CNS function. We assessed a cell's electro-responsiveness through spike discharge, which is the number of action potentials elicited in response to a supra-threshold depolarizing current injection.

The electro-responsiveness of neurons perfused with *B. longum* NCC3001 supernatant (conditioned medium; n = 4) was significantly reduced compared to the control group (those perfused with Krebs solution; n = 5; $P = 0.016$). The electro-responsiveness of neurons perfused

with the conditioned medium was also significantly lower than that of neurons perfused with unconditioned group (MRS growth medium alone) group (n = 4; P = 0.029). In comparing the excitabilities of the neurons in the control group with that of the control media group, there was no statistical difference (P = 0.29).

In subsequent studies, the objective was to identify the AH cells and to determine the effect of *B. longum* NCC3001 conditioned medium on this population of cells. The electro-responsiveness as measured through spike discharge of AH cells perfused with the conditioned medium (n = 5) was significantly reduced compared to neurons perfused with the unconditioned medium (n = 5; P = 0.02). Sensory neurons perfused with the conditioned medium (n = 9) exhibited a significant reduction in their instantaneous input resistances compared to neurons perfused with the unconditioned medium (n = 8; P = 0.01). There was also a significant reduction in the time-dependent input resistance of neurons perfused with the conditioned medium (n = 9) compared to neurons perfused with the unconditioned medium (n = 8; P = 0.02). In addition, perfusion of the conditioned medium over sensory neurons (n = 9) significantly reduced the magnitude of the hyperpolarization-activated cationic current (I_h) compared to neurons perfused with the unconditioned medium (n = 8; P = 0.0003). Furthermore, there was also a significant reduction in the action potential half width duration of myenteric sensory neurons perfused with conditioned medium (n = 5) compared to that exhibited by neurons perfused with the unconditioned medium (n = 5; P = 0.008).

In later experiments, we wanted to gain a more comprehensive understanding of the effect of this bacterium on the gut so we evaluated its effects on the gut musculature. Upon full

immersion, the supernatant of *Bifidobacterium longum* NCC3001 (conditioned medium) caused an initial depolarization of the circular smooth muscle cell. This depolarization continued until the slow wave oscillations in these cells ceased and membrane potential would plateau. Several minutes after this plateau, the slow wave oscillations reappeared and the cell was significantly hyperpolarized relative to the conditions before conditioned medium was added. The resting membrane potential of circular smooth muscle cells in Krebs solution was -54.3 mV and -70.3 mV approximately two minutes after full immersion by the supernatant when the cell was hyperpolarized and a stable recorded was achieved (n = 7; P = 0.02). The average time of onset of depolarization was 18.6 s and the average change in membrane potential (depolarization) from onset of effect to its plateau was 14.0 mV (n = 7). Occasionally, the addition of the conditioned medium only caused an immediate but slight depolarization (n = 3) and in other cases caused only a hyperpolarization of the cell (n = 3) with no significant changes in any slow wave characteristics in either case. Furthermore, any cells that exhibited the waxing and waning of the slow wave lost this pattern upon the addition of the conditioned medium (n = 10).

In attempts to understand the role of neurotransmission in this system, we conducted several experiments whereby carbachol (acetylcholine agonist) and L-NNA (nitric oxide synthase inhibitor) were administered to the muscle. Prior to the addition of 1μM carbachol or $2e^{-4}$ M L-NNA, we would only observe the pacemaker slow wave associated with the interstitial cells of Cajal of the myenteric plexus during the perfusion of Krebs solution. Upon the addition of carbachol (n = 3) or L-NNA (n = 4), we would observe a second slower frequency pattern appear, referred to as a waxing and waning pattern.

ACKNOWLEDGEMENTS

My experiences as a graduate student has invigorated and inspired me to reach for any goal I set my mind to in life. This would not have been possible if it was not for Dr. Jan Huizinga, one of the most passionate researchers that I have ever been blessed to work with. Jan is a brilliant researcher with great ideas and this is well known in the scientific community. His expertise and teaching is second to none and I was incredibly fortunate to be apart of his team. He genuinely showed interest in my ideas and thoughts and always took the time to sit down with me to discuss data and personal dilemmas.

I would also like to thank the members of my supervisory committee, which include Dr. Wolfgang Kunze and Dr. Elena Verdu for their constant support and guidance. Experts in their respective fields, their suggestions and contributions to my study were significant in shaping my project into its final product. Dr Wolfgang Kunze was an integral part of my training because he provided me with valuable technical knowledge and took the time to teach me the fundamentals of enteric neuronal physiology. Dr. Elena Verdu was an essential part of my project because without her I could not attain the bacterial supernatant. I am extremely grateful to all of these individuals for allotting me their time and putting effort into my academic career.

I would also like to thank Dr. Yukang Mao and Dr. Karen-Anne McVey Neufeld for their time and efforts in teaching me the technical skills required for the dissections in my project and also for teaching me the fundamentals of electrophysiology. It was an absolute pleasure working with both of these individuals. In addition, I would like to thank Jun Lu for taking the time out of

her own work to help me purchase and order my mice and my supernatant and her troubles are greatly appreciated.

Finally, I would like to thank the members of my lab past and present, which include Marc Pistilli, George Wright, Dr. Sean Parsons, Dr. Yong Fang Zhu, Dr. Xuan-Yu Wang, Bobbie-Jo Lowie, and Sarah-Lynn Martz for their support on a technical and professional level but also on a more sentimental level. I am humbled to have worked with a group of such talented, bright, and enthusiastic individuals. Dr. Xuan-Yu Wang has been a pivotal part of our lab from a technical aspect and she was always so generous and eager to help with any issues that I had. Dr. Xuan-Yu Wang and Yong Fang Zhu were very generous with their time and efforts in helping me with the neurobiotin injection and visualization of my cells. In addition, I would like to thank my mother, father, and two brothers for their continuous support in all my journeys in life. My parents are my biggest inspiration and have taught me the true value of working hard and obtaining an education and to them I am forever thankful.

TABLE OF CONTENTS

Descriptive Note

Abstract

Acknowledgments

List of Figures

List of Tables

List of Abbreviations

1.0: Introduction

Preface

1.1 Basic functional and structural description of gastrointestinal tract

1.2 Description, distribution, and electrophysiological characteristics of AH neurons

1.3 Functional and morphological specializations of AH neurons

1.4 Significance of AH neurons in gastrointestinal pathophysiology

1.5 Anatomical and functional description of smooth muscle in the small intestine

1.6 Functional description of two ICC networks in the small intestine

1.7 Hypotheses and objectives of thesis

2.0: Effect of *Bifidobacterium longum* NCC3001 on enteric nerve excitability

Preface

2.1 Introduction

2.2 Methods

2.2.1 Tissue preparation

2.2.2 Media preparation

2.2.3 Electrophysiology

2.2.4 Statistical analysis

2.3 Results

2.3.1 Effect of *Bifidobacterium longum* NCC 3001 supernatant on electro-responsiveness of enteric nerves

2.4 Discussion

3.0: The probiotic *Bifidobacterium longum* NCC3001 action on AH cell excitability

Preface

3.1 Introduction

3.2 Methods

3.2.1 Longitudinal muscle-myenteric plexus (LMMP) preparation

3.2.2 Media preparation

3.2.3 Electrophysiology

3.2.4 Neurobiotin injection

3.2.5 Statistical analysis

3.3 Results

3.3.1 Identification of myenteric AH neurons in the mouse ileum

3.3.2 The effect of *Bifidobacterium longum* NCC3001 supernatant on the excitability of myenteric AH neurons in the mouse ileum

3.4 Discussion

4.0: Effect of *Bifidobacterium longum* NCC3001 on slow wave activity of the mouse intestine

Preface

4.1 Introduction

4.2 Methods

4.2.1 Tissue preparation

4.2.2 Media preparation

4.2.3 Electrophysiology

4.2.3 Statistical analysis

4.3 Results

4.3.1 Slow wave activity of the mouse proximal small intestine

4.3.2 The effect of exogenous carbachol and L-NNA on the slow wave activity of the mouse proximal small intestine

4.3.3 The effect of *Bifidobacterium longum* NCC3001 supernatant on the slow wave activity of the mouse proximal small intestine

4.4 Discussion

5.0: General Discussion

5.1 Summary of the major findings of the thesis

5.2 Reflections on the study

5.3 Topics for further research

6.0: References

7.0: Appendices

7.1 List of Publications

LIST OF FIGURES

Figure 1.1 Anatomy of the gut wall

Figure 1.2 The afferent neurons of the digestive tract

Figure 2.1 The effect of *Bifidobacterium longum* NCC3001 on the excitability of myenteric neurons in the mouse ileum

Figure 3.1 AP generated in presence of Krebs solution

Figure 3.2 Excitability measured through spike discharge in myenteric AH neurons recorded using sharp microelectrodes filled with 1 M potassium chloride

Figure 3.3 Digital image of Texas Red fluorescence from an AH neuron that was injected with Neurobiotin dye to reveal its Dogiel type II morphology

Figure 3.4 Bar graphs depicting action potential thresholds, excitabilities, instantaneous input resistances, and time-dependent input resistances of neurons perfused with the conditioned and unconditioned media

Figure 3.5 Contribution of a hyperpolarization-activated cationic conductance (I_H) to the excitability of myenteric AH neurons

Figure 4.1 Pacemaker slow wave recorded from circular smooth muscle of the jejunum in adult mouse

Figure 4.2 Two patterns of frequency measured in the circular smooth muscle of the adult mouse jejunum during the perfusion of Krebs solution using an intracellular microelectrode

Figure 4.3 Two patterns of frequency measured in the circular smooth muscle of the neonatal mouse jejunum during the perfusion of Krebs solution using an intracellular

microelectrode

Figure 4.4 The effect of 1μM carbachol on the two patterns of frequency measured from the circular smooth muscle of the jejunum of an adult mouse

Figure 4.5 The effect of $2e^{-4}$ M L-NNA on the two patterns of frequency measured from the circular smooth muscle of the jejunum of an adult mouse

Figure 4.6 The effect of *Bifidobacterium longum* NCC3001 supernatant on the slow wave activity of the circular smooth muscle of the jejunum of an adult mouse

LIST OF TABLES

Table 3.1 Electrophysiological properties of all recorded myenteric sensory neurons

Table 4.1 Effects of *B. longum* supernatant, carbachol, and nitroarginine on the slow wave characteristics of the mouse jejunum

LIST OF ABBREVIATIONS

5-HT	5-hydroxytryptamine
Ach	Acetylcholine
AH	After-hyperpolarizing
AHP	After-hyperpolarization
BDNF	Brain-derived neurotrophic factor
BK	Calcium-activated potassium channel of large conductance
CCH	Carbachol
CGRP	Calcitonin gene-related peptide
CM	Circular muscle
CO_2	Carbon dioxide gas
DC	Dendritic cell
DSS	Dextran sulfate sodium
EC	Enterochromaffin cell
ENS	Enteric nervous system
ICC	Interstitial cells of Cajal
ICC-DMP	Interstitial cells of Cajal of the deep muscular plexus
ICC-MP	Interstitial cells of Cajal of the myenteric plexus
IK	Calcium-activated potassium channel of intermediate conductance
IP_3	Inositol trisphosphate
IPAN	Intrinsic primary afferent neuron

IR	Immunoreactivity
KCl	Potassium chloride
LM	Longitudinal muscle
LMMP	Longitudinal muscle myenteric plexus
L-NNA	L-NG-Nitroarginine
LPS	Lipopolysaccharide
MRS	de Man, Rogosa and Sharpe growth medium
NO	Nitric oxide
O_2	Oxygen gas
PBS	Phosphate buffered saline
PBS-TX	Phosphate buffered saline-Triton X-100
RMP	Resting membrane potential
S	Synaptic
SCM	Spent culture medium
SK	Calcium-activated potassium channel of small conductance
SP	Substance P

CHAPTER 1: GENERAL INTRODUCTION

PREFACE

The focus of my graduate work has been on investigating the effects of the supernatant of *Bifidobacterium longum* NCC3001 on the excitability of enteric nerves. In addition, I have also investigated the effects of the supernatant on the slow wave activity of the circular muscle layer at the level of the deep muscular plexus (DMP). These efforts would have not been possible if it was not for the technical training I have received from Dr. Kunze, Dr. Mao and Dr. Karen-Anne McVey Neufeld on the fine dissection of a longitudinal muscle-myenteric plexus (LMMP) preparation and training to use the data acquisition systems.

1.1 Basic description of gastrointestinal motility

The human small and large intestine or gut is essentially a hollow, dynamic tube that contracts and relaxes as materials in the lumen of the gut are catabolized and substances are absorbed into the bloodstream. The material in the lumen of the gut can be propelled in anal or oral directions as well as remaining static in one spot of the intestine. The gut wall is composed of several layers that are superposed upon one another: the serosa, the longitudinal muscle layer, the myenteric plexus, the circular muscle layer, the deep muscular plexus, the submucosa, and the mucosa (faces lumen of gut) (Fig 1.1). Contraction and relaxation of the intestine is physically accomplished by the smooth muscle cells in the gut wall, which mechanically drive peristaltic movement and segmentation contractions; together, helping to digest and propel material in the lumen of the gut in an aboral direction. The force, duration, and rate of contraction and relaxation is constantly modulated and regulated by hormonal input, neural

input, and input from pacemaker interstitial cells of Cajal (ICC). Chemical and physical communication among enteric neurons, myenteric pacemaker ICC, and smooth muscle cells, which are all in the gut wall, is essential in maintaining normal, coordinated gastrointestinal motility (*i.e.*, peristalsis and segmentation). Dysfunction of any of these cells that drive normal motility patterns leads to motility patterns in which the propelling of material in the lumen of the gut is either too slow or too rapid (Furness, 2006). The principal type of enteric neuron that most directly determines the patterns of gut motility is the AH neuron.

1.2 Description, distribution, and electrophysiological characteristics of AH neurons

AH neurons are 'sensory' afferent neurons because they sense chemical and physical perturbations inside the lumen of the intestine and, through reflex arcs (intrinsic and extrinsic), can trigger the activation of other neurons, enteroendocrine cells, or smooth muscle cells. For example, an afferent neuron can be stimulated by luminal matter and can send an impulse to interneurons, which then send impulses to inhibitory motor neurons that cause muscles to relax (Fig. 1.2). Anatomically, it has been found that there are more afferent neurons apposed inhibitory motor neurons than there are inhibitory motor neurons with one another (Z. S. Li & Furness, 2000). These sensory neurons are localized to networks of ganglia that in the myenteric plexus, which is a plexus that is located between the circular and longitudinal muscle layers of the gut wall. These neurons are connected in series with other neurons and respond in a hierarchical fashion. The first neuron in this hierarchy is the primary afferent neuron, which has varicosities that extend all the way into the epithelial cells lining the lumen of the gut. These varicosities are filled with acetylcholine, calcitonin-gene related peptide (CGRP), and substance

P, which diffuse to other neurons or smooth muscle cells. Consequently, primary afferent neurons are located closest to the lumen of the gut as compared to other enteric neurons. These primary afferent neurons are proceeded by the secondary neurons in series, and then to

Fig. 1.1 The anatomy of the gut wall. The basic tissue layers of the gastrointestinal tract are represented with the location of select populations of interstitial cells of Cajal. From the gut lumen, the layers include: the musoca, submucosa, deep muscular plexus, inner circular muscle layer, myenteric plexus, longitudinal muscle layer, and serosa (White *et al*., 2008).

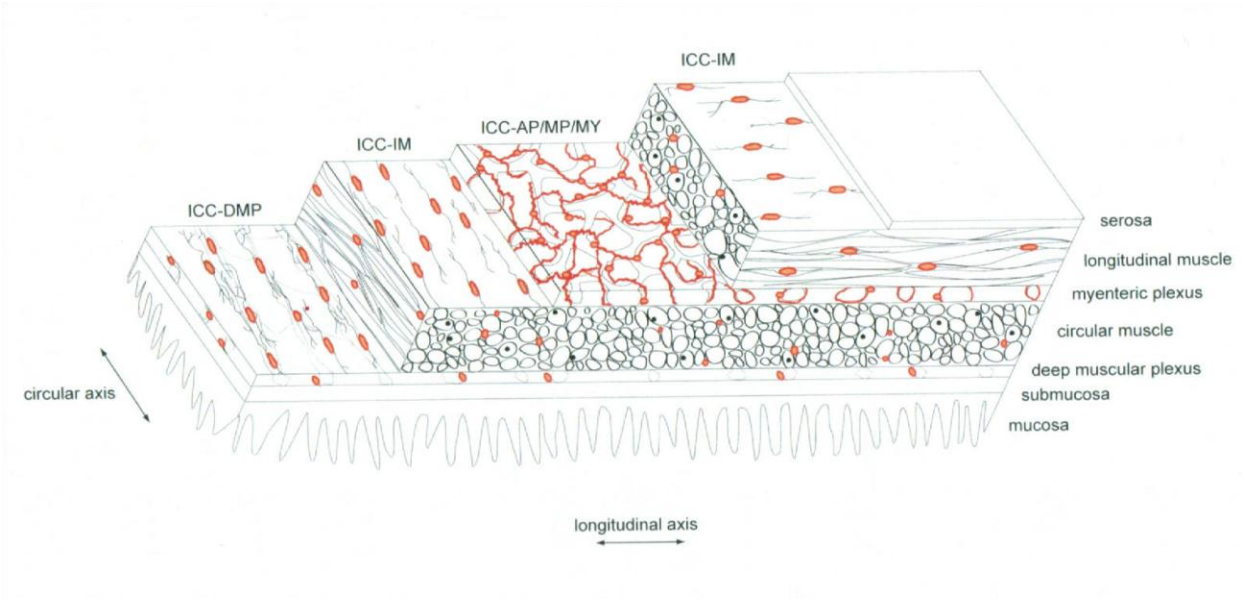
ICC-IM
ICC-AP/MP/MY
ICC-IM
ICC-DMP
serosa
longitudinal muscle
myenteric plexus
circular muscle
deep muscular plexus
submucosa
mucosa
circular axis
longitudinal axis

higher order neurons. Furthermore, there are two classes of primary afferent neurons: intrinsic primary afferent neurons (IPANs) and extrinsic primary afferent neurons. IPANs have their somas, processes, and synaptic connections within the gut wall, whereas extrinsic primary afferent neurons have their somas in nodose and jugular ganglia or in dorsal ganglia (Fig. 1.2) (Furness, 2006). AH neurons are electrophysiologically distinct from other neurons in two significant manners. Firstly, these neurons possess an inflection (hump) on the falling phase of their action potentials as measured in the guinea pig, the rat (W. A. Kunze et al., 2009), and in the mouse small intestine (Mao, Wang, & Kunze, 2006). Secondly, the action potentials generated by an AH neuron is also characterized by a two phase after-hyperpolarization (AHP): a fast AHP and a slow AHP. This characteristic is also measurable from AH neurons in guinea pigs, rats (W. A. Kunze et al., 2009), and mouse species (Mao et al., 2006). An action potential is triggered in an AH neuron once the cell becomes depolarized (net gain of positive charge or net loss negative charge) up until the threshold for activation of an action potential is reached (Hillsley, Kenyon, & Smith, 2000; W. A. Kunze et al., 2009; Mao et al., 2006). Depolarization of an AH neuron leads to the activation of voltage-activated sodium and calcium ion channels (N-type calcium ion channel; (Rugiero et al., 2002), which allow an influx of sodium and calcium ions, respectively, from the extracellular fluid. This influx of calcium then initiates a calcium induced calcium release (CICR) from the sarcoplasmic reticulum through the IP_3 and ryanodine-sensitive receptors (Hillsley et al., 2000), which increases the already high intracellular calcium concentration. This accumulation of calcium ions within the cytosol leads to the activation of ligand (calcium) – gated potassium channels (SK channels: small conductance; IK channels:

intermediate conductance; and BK channels: big conductance). Once activated, these potassium ion channels allow the efflux of potassium ions from the cytosol of the nerve to the extracellular fluid (Hillsley et al., 2000; Mao et al., 2006; Vanden Berghe, Kenyon, & Smith, 2002). This last phase causes the neuron to become hyperpolarized (net loss of positive charged; loss of K^+) with respect to its membrane potential (difference in ionic charge across plasma membrane), which allows intracellular ionic concentrations to revert to resting levels. Big- and intermediate-conductance calcium activated potassium channels (BK channels & IK channels) are responsible for the fast and slow AHP, respectively (Furness et al., 2004). These ligand-gated ion channels are particularly interesting because it is hypothesized that the excitability of AH neurons relies on the level of activity of the late AHP current, both at rest and following an AHP (Furness, 2006). Moreover, in both the guinea pig (Z. S. Li & Furness, 2000) and mouse ileum (Mao et al., 2006), all AH neurons displayed Dogiel type II morphology, which is characterized by a round or oval cell body with several dendrites and one axon (Dogiel, 1895, 1899).

Fig. 1.2 The afferent neurons of the digestive tract. Two classes of intrinsic primary afferent neurons (IPANs) exist: myenteric IPANs, which respond to distortion of their processes in the external muscle layers and, via processes in the mucosa, to changes in luminal chemistry, and submucosal IPANs that detect mechanical distortion of the mucosa and luminal chemistry. Intrinsic primary afferent neurons have their somas, processes, and synaptic connections within the gut wall, whereas extrinsic primary afferent neurons have their somas in nodose and jugular ganglia or in dorsal ganglia. LM, longitudinal muscle; MP, myenteric plexus; CM, circular muscle; SM, submucosa; MU, mucosa (Furness, 2000; adapted from Furness *et al*., 2004).

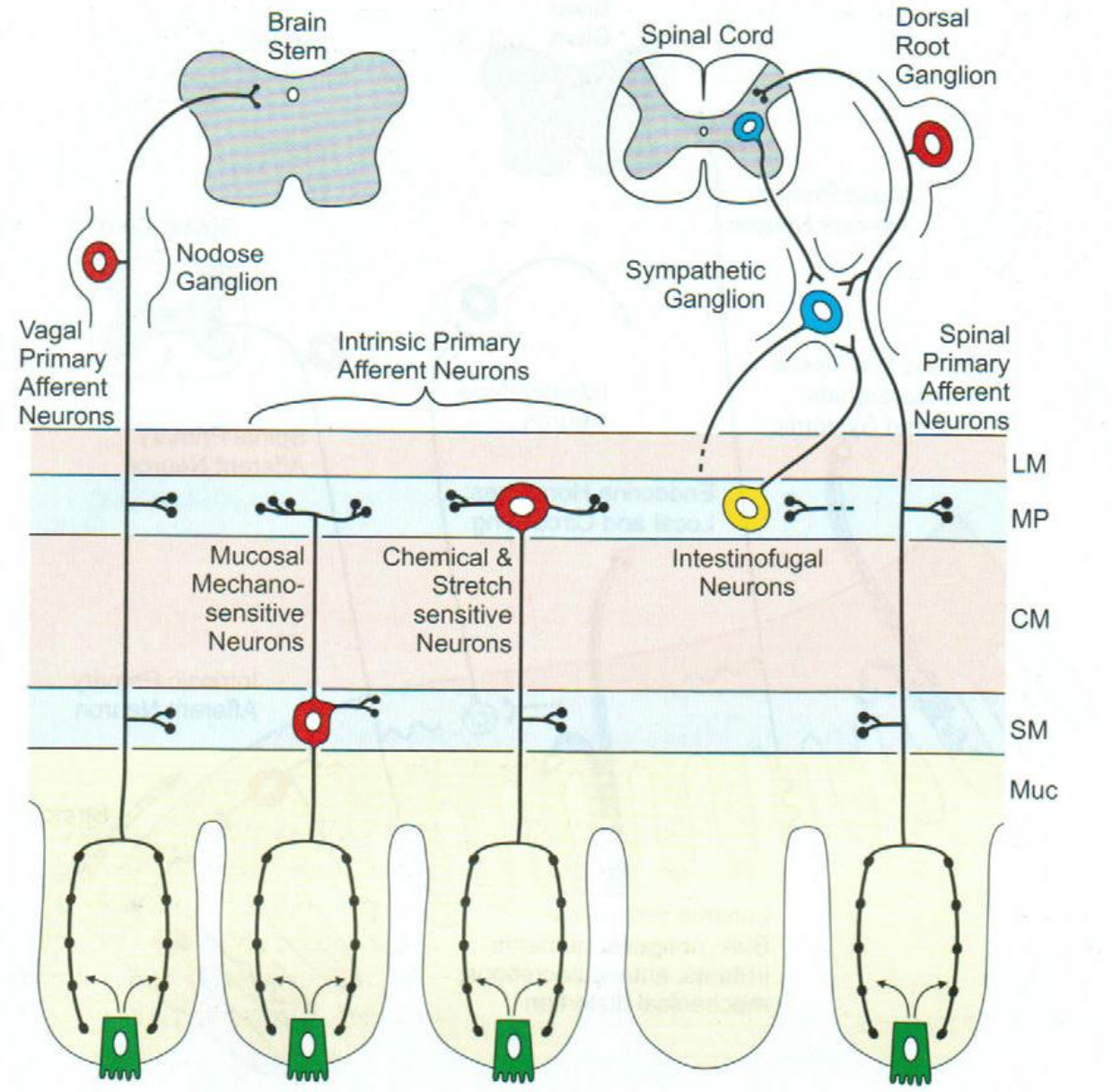
Brain Stem
Spinal Cord
Dorsal Root Ganglion
Nodose Ganglion
Sympathetic Ganglion
Vagal Primary Afferent Neurons
Intrinsic Primary Afferent Neurons
Spinal Primary Afferent Neurons
LM
MP
CM
SM
Muc
Mucosal Mechano-sensitive Neurons
Chemical & Stretch sensitive Neurons
Intestinofugal Neurons

1.3 Functional and morphological specializations of AH neurons

IPANs can receive synapses from adjacent neurons on their soma and on the proximal regions of their processes (Pompolo & Furness, 1988). These neurons only respond to stimuli that are at the threshold level of evoking a reflex (Gershon & Kirchgessner 1991). In addition, there are two further subdivisions associated with IPANs: myenteric IPANs and submucosal IPANs (Fig. 1.2). Myenteric IPANs respond to the distortion of their processes in external muscle layers and in the mucosa to luminal chemistry (W. A. A. Kunze, Furness, Bertrand, & Bornstein, 1998; W. A. A. Kunze, Clerc, Furness, & Gola, 2000; Mao et al., 2006), whereas submucosal IPANs detect mechanical distortion and the luminal chemistry of the mucosa (Furness, Alex, Clark, & Lal, 2003; Furness et al., 2004). Furthermore, there are also IPANs that detect chemical stimuli presented on the mucosa surface facing the lumen as observed in the guinea pig small intestine using intracellular electrodes (Bertrand, Kunze, Bornstein, Furness, & Smith, 1997; W. A. A. Kunze, Bornstein, & Furness, 1995). Additionally, it has been found that capsaicin, which is the pungent component of chilli peppers that humans perceive as spiciness, causes the release of smooth muscle relaxant substances from afferent nerve endings in human sigmoid colon circular muscle strips (Bartho, Benko, Lazar, Illenyi, & Horváth, 2002). When glucose was presented on the mucosal side of intestinal tissue, both myenteric and submucosal IPANs were activated (A. L. Kirchgessner, Liu, & Gershon, 1996). Some IPANs can turn distortions of their processes into firing action potentials when their myenteric processes are physically pressed upon. These IPANs do so using mechanosensitive ion channels and collagen fibre connections linking their processes to muscle (W. A. A. Kunze et al., 1998; W. A. A.

Kunze & Furness, 1999; W. A. A. Kunze, Clerc, Bertrand, & Furness, 1999; W. A. A. Kunze et al., 2000). In support of this phenomenon that IPANs have the ability to turn distorted processes into fired action potentials is the fact that when muscle relaxants were absorbed, action potentials were terminated. Also, after being exposed to proteolytic enzymes that breakdown the connective tissue connecting an IPAN to a muscle, an IPAN elicited no more activation (W. A. A. Kunze et al., 1999).

1.4 Significance of AH neurons in gastrointestinal pathophysiology

As mentioned previously, the excitability of an AH neuron relies on the level of activity of the slow AHP current (at resting and excited states) (Furness, 2006). In order for an action potential to fire, the neuron needs to become depolarized and reach its threshold of activation. However, it is the degree to which the slow AHP has hyperpolarized the cell from the previous action potential firings that determines whether it will become sufficiently depolarized to fire subsequent action potentials. This supports the notion that the excitability of an AH neuron is directly proportional to the number of action potentials that it fires (Hillsley et al., 2000; Vanden Berghe et al., 2002) because in order for repetitive action potentials to fire (*i.e.*, repetitive threshold activations) the cell needs to be in a relatively depolarized state after the slow AHP from the previous action potential. Consequently, it is the calcium activated potassium ion channels and the intracellular calcium concentration that directly determine the excitability of an AH neurons since it is the high intracellular calcium concentration that activates the potassium ion channels. From a pharmacological aspect, gastrointestinal motility disorders can be treated with drugs that target either structures that release calcium into the cytosol or those that target

calcium activated potassium ion channels, which together significantly influence AH neuron excitability. Any changes to an AH neuron's excitability means that there will be changes in the rate in which the neuron stimulates other neurons (including descending interneurons & inhibitory motor neurons), smooth muscles, among other cell types. All of these changes mean changes in the rate at which luminal material is digested and propelled. TRAM-34, a calcium activated, intermediate conductance potassium ion channel (IK channel) blocker, resulted in a complete abolishment of fluid propulsion in the rat small intestine, *in vivo* (Ferens, Baell, Lessene, Smith, & Furness, 2007). By aiming to adjust the sensitivity (excitability) of 'sensory' afferent neurons, then a treatment for gastrointestinal motility disorders can be a possible implication.

1.5 Anatomical and functional description of smooth muscle in the small intestine

The population of cells responsible for the mechanical force driving propulsive motility are the rings of circular smooth muscle cells lining the gut wall. Circular smooth muscle cells of the murine small intestine are located between the myenteric plexus (MP) and the submucosa. The circular smooth muscle layer consists of a thin sheet of circular smooth muscle cells that lays atop the deep muscular plexus (DMP), underneath which is the bulk of the circular smooth muscle cells. The DMP contains a collection of enteric nerve fiber bundles and interstitial cells of Cajal. In this plexus, the interstitial cells of Cajal demonstrate synaptic like junctions with the enteric nerves that innervate this region (X. Y. Wang, Paterson, & Huizinga, 2003). These nerve bundles are distributed in networks that are circumferentially oriented and travel along the intestine (Furness, 2006). The interstitial cells of Cajal play an important role in this region,

hypothesized to act as intermediaries in the communication between enteric neurons and smooth muscle cells in the DMP (Ward, McLaren, & Sanders, 2006).

It is well established that the interstitial cells of Cajal associated with the myenteric plexus (ICC-MP) are the pacemaker cells of the small intestine, rhythmically oscillating intracellular calcium and through this a generation of a basic electrical rhythm (BER). This electrical rhythm dictates the frequency of peristaltic motor activities (Huizinga et al., 1995; Lowie, Wang, White, & Huizinga, 2011) and is referred to as the pacemaker potential (Kito & Suzuki, 2003). The pacemaker potential creates an electrotonic potential that passes to neighbouring circular and longitudinal smooth muscle cells (Kito & Suzuki, 2003; Kito, Ward, & Sanders, 2005) likely through gap junctions that connect myenteric interstitial cells of Cajal with one another and with the circular smooth muscle layer (Daniel, Wang, & Cayabyab, 1998). It has been described previously that the slow waves of the smooth muscle are maximal in amplitude in cells that are nearest to the ICC-MP (Suzuki, Prosser, & Dahms, 1986). The electrical potential experienced by the smooth muscles is referred to as the slow wave (Kito & Suzuki, 2003), which drives the membrane potential fluctuations of the smooth muscle cells due to local ionic imbalances. If the slow wave of a smooth muscle cell is superimposed by an excitatory stimulus, such as through a connection with an excitatory nerve, then the muscle cell will depolarize and subsequently contract if the threshold of L-type calcium channel activation is reached (Malysz, Richardsons, Farraway, Huizinga, & Christen, 1995). When the smooth muscle slow wave is superimposed with spike potentials it will contract and in this instance there will be propulsive contractions that will propel luminal content aborally and cause outflow (Donnelly et al., 2001;

Huizinga, Ambrous, & Der-Silaphet, 1998b). This mechanism is the basis of all propulsive peristaltic motor activities of the small intestine.

The slow wave frequency of the small intestine is paced with a gradient; higher frequencies appear in the proximal small intestine and decreases aborally (Chen, Schirmer, & McCallum, 1993). One author referred to the regions of intestine that have the same frequency as displaying frequency plateaus (Diamant & Bortoff, 1969). This slow wave gradient is also representative of the transit gradient of the small intestine where intestinal content has a more rapid transit in the proximal small intestine as compared to its distal end (Der-Silaphet, Malysz, Hagel, Arsenault, & Huizinga, 1998b).

Of the literature that investigate the slow wave activity of the small intestine, fewer describe a pattern referred to as waxing and waning, which is when the slow wave amplitude modulates by increasing and decreasing in size (Chang et al., 2001; Der-Silaphet, Malysz, Hagel, Arsenault, & Huizinga, 1998a; Diamant & Bortoff, 1969; Hudson, Mayhew, & Pearson, 2001). One earlier researcher described this waxing and waning as an interference event resulting from the differences in slow wave frequencies of adjacent cell populations (Diamant & Bortoff, 1969).

1.6 Functional description of two ICC networks in the small intestine

The interstitial cells of Cajal of the myenteric plexus (ICC-MP) are the pacemaker cells of the gastrointestinal system (Huizinga et al., 1995). They rhythmically oscillate intracellular calcium (Torihashi, Fujimoto, Trost, & Nakayama, 2002; Yamazawa & Iino, 2002) and create electrical waves called pacemaker potentials (Kito & Suzuki, 2003) at approximately the same frequency to this calcium oscillation (Park et al., 2006). This pacemaker potential is the basic

electrical rhythm (BER) of the gastrointestinal tract and the fundamental component in all peristaltic motor patterns. This electrical rhythm is abolished in W/W^v mice, which are selectively deficient in ICC-MP (Nakagawa, Misawa, Nakajima, & Takaki, 2005). Since ICC-MP propagate slow waves to the muscle, coordinated smooth muscle contraction is largely dependent on ICC-MP in helping to drive the membrane potential closer to the activation of L-type calcium channels. Hence, slow wave activities were abolished in W/W^v mice and outflow of intraluminal content in these mice was not observed (Huizinga, Ambrous, & Der-Silaphet, 1998a). In a further study, it was nicely shown that the slow waves propagated by the ICC-MP were required to cause a net propulsive effect of contractile activity through the use of wild-type and ICC-MP knockout mice (Der-Silaphet, Malysz, Hagel, Arsenault, & Huizinga, 1998a). The interstitial cells of Cajal of the myenteric plexus have been well characterized and their intrinsic ability to oscillate electrically allows them to function as the pacemaker cells of the gastrointestinal tract.

Another population of interstitial cells of Cajal are positioned in the deep muscular plexus (ICC-DMP) and have been attributed an intermediate role in the communication between enteric motor neurons of this plexus to adjacent muscle cells. Some studies revealed that ICC-DMP demonstrate synapse-like junctions with nerve varicosities in the DMP (Rumessen, Mikkelsen, & Thuneberg, 1992; X. Y. Wang et al., 2003). It was also shown that neural responses to electrical field stimulation (EFS) of circular smooth muscle cells were poorly developed in mice immediately after birth, which is a time when ICC-DMP are not fully developed. At 10 days post partum (P10), when ICC-DMP are developed, cholinergic and

nitrergic neural responses were fully integrated in response to EFS (Ward et al., 2006). In the small intestine, ICC-DMP do not play a role in the intrinsic slow wave propagation in the gastrointestinal tract as W/W^v mice still retain an ICC-DMP network but do not propagate slow waves (Nakagawa et al., 2005). In one fascinating study, a *T. spiralis* infection was associated with loss of interstitial cells of Cajal and enteric neurons of the DMP and also associated with a loss of the waxing and waning pattern, which was induced by distension. Interestingly, a resolution of the infection lead to a recovery of the interstitial cells of Cajal of the deep muscular plexus (ICC-DMP) and of the waxing and waning (X. Y. Wang et al., 2005).

1.7 Hypotheses and objectives of thesis

We hypothesize that *Bifidobacterium longum* NC 3001 metabolites alter the excitability of myenteric sensory neurons (AH/ Dogiel type II neurons) in the ileum of the mouse. We quantified excitability by assessing a cell's threshold and electro-responsiveness, which is the number of action potentials elicited in response to a 500 ms supra-threshold depolarizing current injection (*i.e.,* spike discharge) with an intensity equal to rheobase (threshold) plus 50 pA (picoamperes). Threshold refers to the intensity of current that is required to elicit one action potential (AP). The specific objective is:

1) To perfuse an LMMP preparation of the mouse ileum with the Krebs solution buffer, the conditioned medium, and the unconditioned medium to investigate the supernatant's effect(s) (if any) on the excitability of myenteric AH neurons using an intracellular microelectrode to detect electrical changes in membrane potential.

We also hypothesize that the propulsive motor pattern of the mouse small intestine is stimulus-dependent; in other words, a stimulus (*e.g.*, distension) is needed to initiate the propulsion of the gut luminal content in an anal direction, which are mechanically driven by rings of circular smooth muscle. The specific objective is:

1) To measure and record membrane potentials experienced by circular smooth muscles near the deep muscular plexus using an intracellular microelectrode.
2) To study the effects of *Bifidobacterium longum* NCC3001 as well as various pharmacological agents that mimic neurotransmission in the gastrointestinal tract, such as exogenous CCh and L-NNA, on the musculature of the small intestine.

CHAPTER 2.0: EFFECT OF *BIFIDOBACTERIUM LONGUM* NCC3001 ON ENTERIC NERVE EXCITABILITY

PREFACE

The initial interest in *Bifidobacterium longum* NCC3001 stemmed from a study from the Bercik research group that revealed that it can normalize anxiety-like behaviour and hippocampal BDNF levels after parasitic infection with *T. muris*. Therefore, we set to investigate the possible route whereby this communication between the gut and the brain can occur by investigating a fundamental premise, which was that the products released by the probiotic may potentially act first on enteric neurons, which subsequently communicate through neuon-neuronal interaction with the brain.

2.1 Introduction

The research group of Bercik at McMaster University conducted a study that has been accepted for publication entitled **the anxiolytic effect of *Bifidobacterium longum* NCC3001 involves vagal pathways for gut-brain communication.** This chapter reports on the contribution I made to this study.

The probiotic *Bifidobacterium longum* NCC3001 has been shown to normalize anxiety-like behaviour and hippocampal brain derived neurotropic factor (BDNF) levels in mice infected with *Trichuris muris* in a model of infectious colitis (Bercik et al., 2010). Utilizing a chronic model of colitis, a study was conducted to decipher whether or not the anxiolytic effects of *Bifidobacterium longum* NCC3001 involved the vagus. Mice in an experimental group were given drinking water contaminated with 3% dextran sodium sulfate (DSS) for 3 cycles, each one week in duration, with age-matched controls given normal drinking water throughout the entire study. Placebo were either gavaged with live *B. longum* NCC3001 or growth medium alone during the last 7 day cycle of DSS. To determine the role of vagal integrity in the interaction between the gut and the brain in this model of chronic colitis, one group of mice were vagotomized and allowed to recover over a 7 day period before DSS treatment. At the end of the last cycle of DSS, behaviour was assessed by step-down and light preferences tests. To investigate the mechanism of action of *B. longum* NCC3001 in this chronic model of colitis, the exact protocols for colitis induction and probiotic/placebo treatment were conducted on mice in a separate group that underwent subdiaphragmatic vagotomy and surgical widening of the opening of their pylorus 2 days after the end of the second cycle of DSS. At the end of the last cycle of DSS, behaviour in this group was assessed by using step-down and light preferences test. The

mice were sacrificed 24 hours later, where colonic tissues were sampled for inflammation by myeloperoxidase activity (MPO) and histology. Also, BDNF mRNA was measured in human SH-SY5Y neuroblastoma cells after being incubated with the sera from *B. longum*- or placebo-treated mice.

My specific contribution to this study was an assessment of the effect of *B.longum* NCC3001 on enteric neuron excitability. My specific objective was to find evidence for interaction between *B.longum* NCC3001 and myenteric neurons as a potential route for *B.longum* NCC3001 to influence CNS function. This was conducted by taking microelectrode recordings of electrical changes in membrane potentials of exposed myenteric neurons exposed to Krebs solution, the conditioned or unconditioned media.

In this model of chronic colitis, the induced disease was associated with anxiety-like behaviour, which was absent in vagotomized mice. The probiotic *Bifidobacterium longum* NCC3001 normalized behaviour but had no effect on MPO activity or histological scores. The anxiolytic effects of this probiotic were absent in anxious mice that were later vagotomized before the last cycle of DSS. *B.longum* NCC3001 metabolites did not have an effect on BDNF mRNA expression in human SH-SY5Y cells but did, however, lower the excitability of myenteric neurons, which may communicate with the CNS by interacting with vagal pathways that innervate the enteric nervous system.

2.2 Methods

2.2.1 Tissue preparation

All experiments were performed on sections of ileum excised from adult (6-8 week old) male AKR mice (The Jackson Laboratory, Bar Harbor, ME) immediately after the animal was sacrificed via cervical dislocation. The segments were placed in a recording dish lined with Sylgard® gel and opened along the length of the mesenteric border and pinned flat under sufficient tension with insect pins with the mucosa facing upwards. During tissue preparation, the ileal segment was constantly submerged in Krebs solution (composition (in mM): NaCl (118.1), NaH_2PO_4 (1.0), $MgSO_4$ (1.2), $CaCl_2$ (2.5), KCl (4.8), glucose (11.1), $NaHCO_3$ (25)) and maintained at room temperature while constantly oxygenated with a gaseous mixture of 95% O_2-5% CO_2. 2 µM of nicardipine (L-type calcium channel blocker) and 1 µM of scopolamine (muscarinic receptor antagonist) were added to the Krebs solution to prevent tissue contraction. Once the tissue was pinned down, a longitudinal muscle myenteric plexus (LMMP) preparation was made using a pair of fine dissection forceps; the mucosa, submucosa, deep muscular plexus, and circular muscle layers were carefully removed to expose the myenteric plexus. The recording dish was then placed on the recording chamber of a high powered inverted microscope (Zeiss Axiovert S100 TV) and continuously perfused (4 mL/ min.) with the prepared Krebs solution that has been heated to 37^{o}C via a water bath-heat exchange system.

2.2.2 Media preparation

Bifidobacterium longum NCC3001 was obtained from Nestlé Culture Collection (Lausanne, Switzerland) and cultured for 24 hours at 37°C under anaerobic conditions in de Man–Rogosa-Sharpe (MRS; unconditioned medium) broth containing 0.5% cysteine. The bacterial cells were separated by centrifugation for 15 minutes at 5000*g* at 4°C, resuspended

again at a concentration of 10^{10} cells/ mL in their spent culture medium. Samples were kept in frozen (-80°C) aliquots until ready for use. The probiotic was prepared as previously described (Verdú et al., 2004). Before use, aliquots were filtered through a 0.2 µM filter to obtain bacteria-free conditioned medium (supernatant).

A dilution was then prepared containing Krebs solution (containing 2 µM nicardipine and 1 µM scopolamine) and either the conditioned medium or unconditioned medium in a 20:1 ratio, respectively, under sterile conditions in a biological safety cabinet, oxygenated with a gaseous mixture of 95% O_2-5% CO_2 throughout the entire length of the experiment.

2.2.3 Electrophysiology

All preparations were allowed to equilibrate in Krebs solution for at least one hour prior to recording. Neurons were impaled with conventional borosilicate glass micropipettes (fire polished; length: 7 cm; O.D: 1.5 mm; I.D: 0.86 mm) filled with 1 M KCl and fabricated to yield resistances between 100-120 MΩ. Recordings were made using a MultiClamp 700B amplifier (Axon Instruments). Signals were digitized using a Digidata 1322A acquisition system (Axon Instruments) and stored on the PC. Neuronal excitability (electro-responsiveness) was assessed by injecting a 500 ms depolarizing current with a magnitude equal to rheobase plus 50 pA once every 10 seconds. Electro-responsiveness is expressed as the number of action potentials a neuron fires in response to a depolarizing current injection with supra-threshold intensity.

2.2.4 Statistical analysis

Data were compared using the Mann-Whitney U-test ($p < 0.05$).

2.3 Results

2.3.1 Effects of *Bifidobacterium longum* NCC 3001 supernatant on electro-responsiveness of enteric nerves

The perfusion of the supernatant (conditioned medium) from *Bifidobacterium longum* NCC 3001 over enteric neurons decreased the excitability of these neurons compared to that of neurons perfused with either the Krebs solution or the unconditioned medium (Fig. 2.1). The electro-responsiveness of neurons in the control group (those perfused with Krebs solution) was 3.95 $\pm$ 4.16 (mean $\pm$ SD; n=5) versus the electro-responsiveness of neurons perfused with the conditioned medium, which was 0.25 $\pm$ 0.50 (n=4; p = 0.016). The electro-responsiveness of neurons in the unconditioned group (de Man, Rogosa, Sharpe growth medium alone) was 1.68 $\pm$ 0.94 (n=4), significantly different from the supernatant group (p = 0.029). In comparing the excitabilities of the neurons in the control group with that of the control media group, there was no statistical difference (p = 0.29). The instantaneous input resistance of the control group was 131 $\pm$ 70, of the supernatant group, 87 $\pm$ 56 (p = 0.41). The instantaneous input resistance of the supernatant group was not statistically different from that of the control media group, (175 $\pm$ 97; p = 0.11).

Fig. 2.1 The effect of *Bifidobacterium longum* NCC3001 on the excitability of myenteric neurons in the mouse ileum. The effect of the supernatant from *Bifidobacterium longum* NCC 3001 on the excitability of enteric neurons. *A*: A digital image of an individual neuron within a ganglion being impaled with an intracellular microelectrode (*in white*). *B*: Intracellular microelectrode recording using a pipette filled with 1 M KCl. Action potential discharge on injection of a 500 ms duration current pulse (*B'*) with a 350 picoampere (pA) intensity. This neuron fired two action potentials in response to a supra-threshold current pulse set at threshold plus 50 millivolts (*B inset*). *C*: No action potentials were discharged from this neuron after the injection of a 500 ms duration current pulse (*C'*) with a 450 pA intensity. *D*: action potential discharge on injection of a 500 ms duration current pulse (*D'*) with a 400 pA intensity. This neuron fired one action potential in response to a supra-threshold pulse set at threshold plus 50 millivolts (*D inset*).

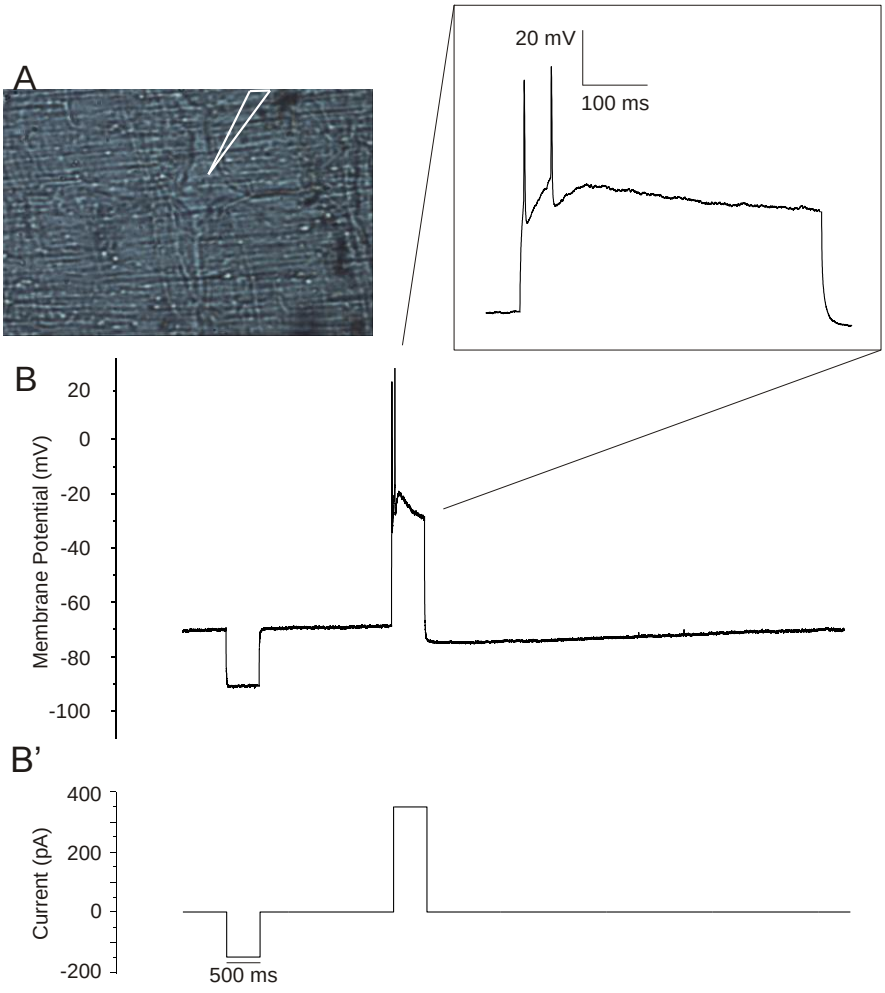
A
20 mV
100 ms
B
Membrane Potential (mV)
20
0
-20
-40
-60
-80
-100
B'
Current (pA)
400
200
0
-200
500 ms

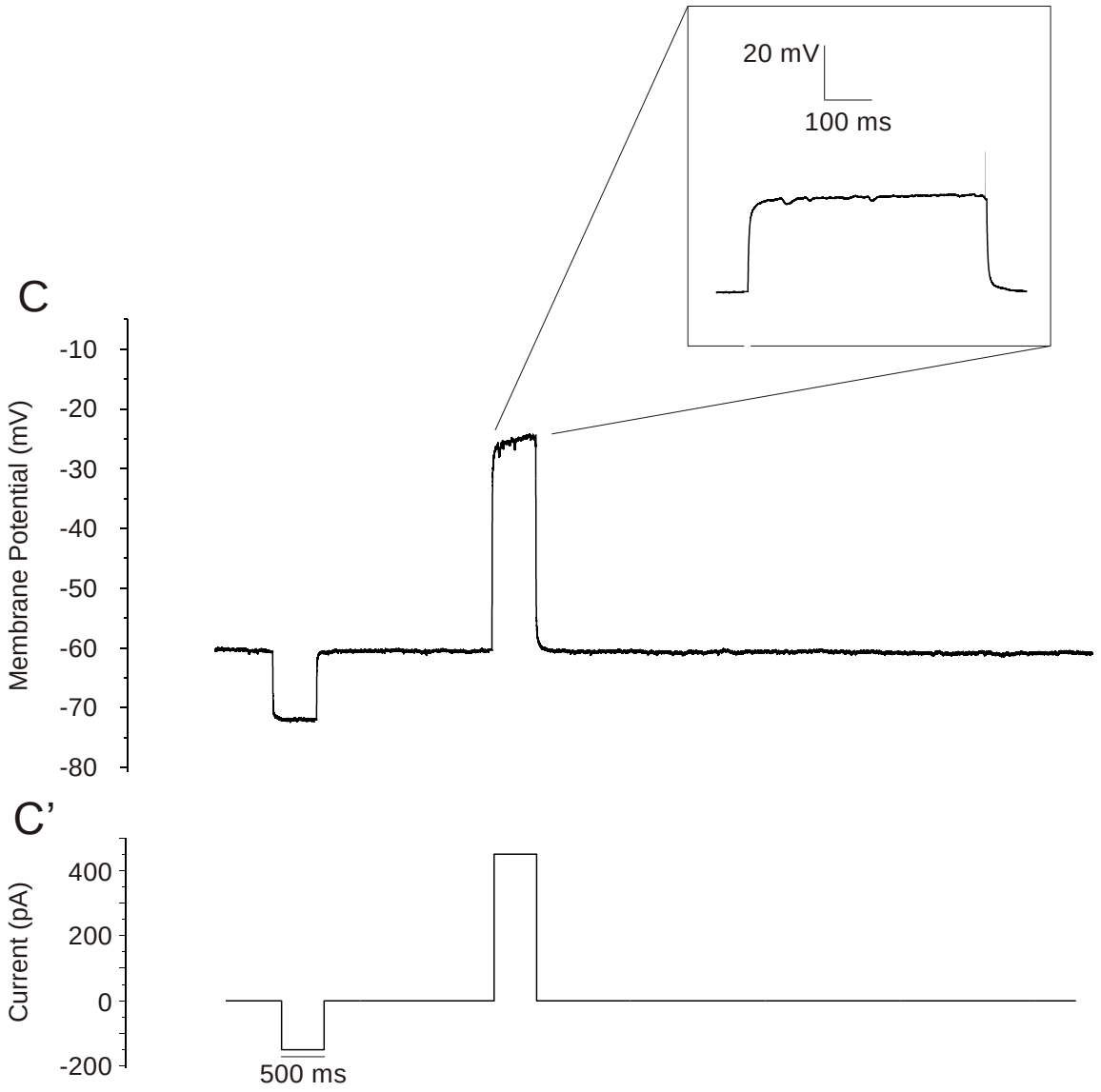
20 mV
100 ms
C
-10
-20
-30
-40
-50
-60
-70
-80
Membrane Potential (mV)
C'
400
200
0
-200
Current (pA)
500 ms

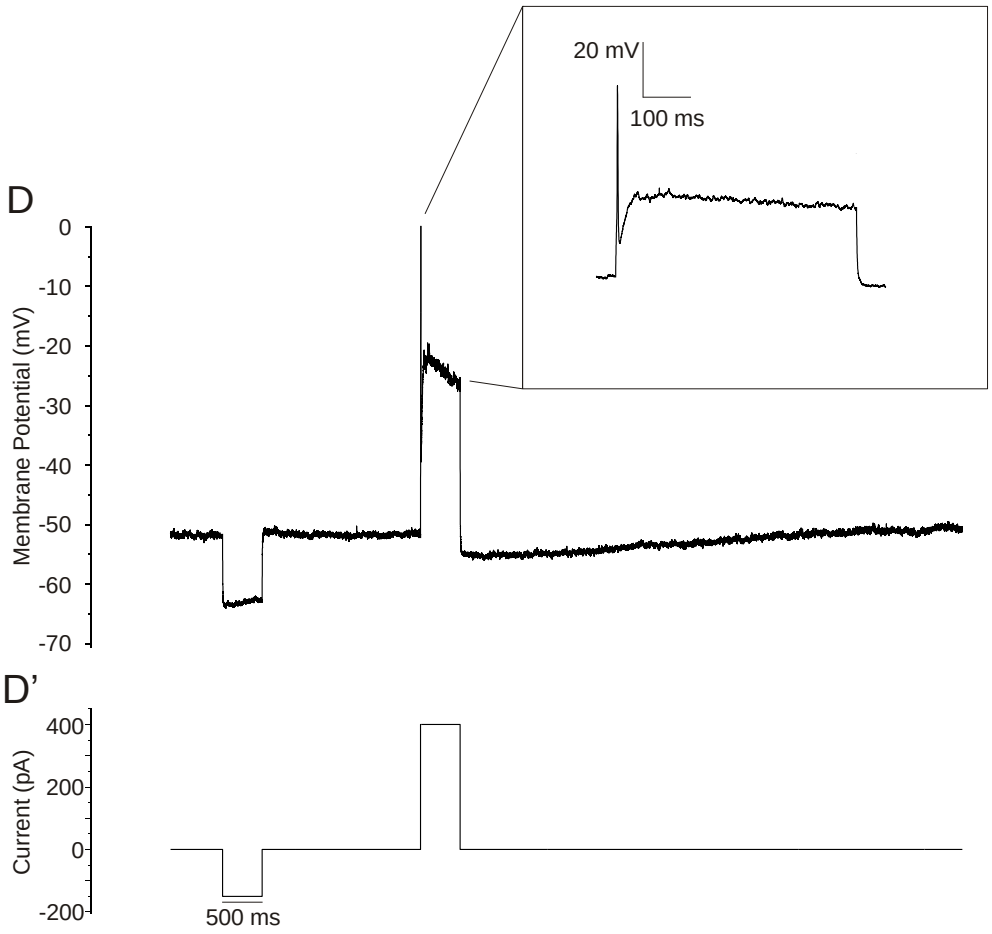
D
20 mV
100 ms
0
-10
-20
-30
-40
-50
-60
-70
Membrane Potential (mV)
D'
400
200
0
-200
Current (pA)
500 ms

2.4 Discussion

The supernatant from *Bifidobacterium longum* NCC 3001 decreased the excitability of enteric neurons in the small intestine of the mouse. The *in situ* recordings allow us to assess neuron function in an environment that is as close to physiological as possible (Mao et al., 2006). A possible explanation for the fact that virtually no action potentials were fired from neurons in the presence of the supernatant from *Bifidobacterium longum* NCC 3001 is that a particular metabolite synthesized by this probiotic inhibits sodium and/or calcium channels.

CHAPTER 3.0: THE PROBIOTIC *BIFIDOBACTERIUM LONGUM* NCC3001 ACTION ON AH CELL EXCITABILITY

PREFACE

Myenteric AH neurons are the only chemosensory afferent neurons of the enteric nervous system and therefore a perfect candidate to test the effects of *Bifidobacterium longum* NCC3001 since in a physiological setting this probiotic would secrete metabolites which can indirectly interact with AH neurons via absorption through mucosal epithelial cells or absorption into the blood stream and as well through direct contact with the terminal ends of AH cells after absorption through the mucosal epithelial cells. The action of any substance on AH cells may have implications in gut motility since AH cells form intrinsic reflexes with enteric motor neurons.

3.1 Introduction

Probiotics are live microorganisms that promote beneficial effects on their host through continuous administration (Fioramonti, Theodorou, & Bueno, 2003). These commensal

organisms have been described to adequately reduce visceral hypersensitivity to perturbations of the gastrointestinal tract in mice and rats (Kamiya et al., 2006; Verdu et al., 2006) and moderate small bowel (B. Wang, Mao et al., 2010) and large bowel motility (W. A. Kunze et al., 2009; B. Wang, Mao, Diorio, Wang, Huizinga et al., 2010a). The probiotic *Bifidobacterium longum* NCC3001 has been shown to normalize anxiety-like behaviour in mice infected with *Trichuris muris* (Bercik et al., 2010). An unresolved issue from this study was how *B. longum* interacted with the nervous system. Our hypothesis was that the first contact was with AH neurons.

Intrinsic primary afferent neurons or after-hyperpolarizing (AH) neurons (Hirst, Holman, & Spence, 1974) are at the afferent end of reflex arc networks in the enteric nervous system (ENS) and reside in the myenteric plexus (Furness, 2006). They are the first population of neurons (Furness, 2006) in the afferent hierarchy of intrinsic neurons innervating the gut and can 'sense' chemical and physical disruptions in the gut lumen through long processes that extend from their somas in the myenteric plexus and submucosa close to epithelial cells (Bertrand, Kunze, Furness, & Bornstein, 2000). AH neurons contain excitatory and inhibitory neurotransmitters and, depending on the type of signal that they receive from stimuli, they send either excitatory or inhibitory signals to other neurons and smooth muscle cells by means of action potential propagation and subsequent neurotransmitter release (W. A. A. Kunze & Furness, 1999). It is highly likely that these neurons receive stimuli (e.g., metabolites, cellular debris, etc.) from the bacteria that colonize the gut and therefore it is plausible that these bacteria can alter gut motility through direct or indirect actions on neurons, smooth muscle cells, and interstitial cells of Cajal. The present study was undertaken to assess and characterize the effects

of *Bifidobacterium longum* NCC3001 supernatant on the excitability of myenteric AH cells (sensory neurons).

Probiotics, once in the lumen, produce small molecules that may contribute significantly to their mode of action (Antunes, Davies, & Finlay, 2011). These small molecules may travel to the blood stream and in this way gut bacteria have a large effect on the composition of blood metabolites (Wikoff et al., 2009) and hence through this route can exert powerful effects on the host. Blood metabolites have access to the myenteric plexus of the gut, which is heavily vascularized where they can act on all cells including intrinsic and extrinsic neurons, glial cells, ICC and smooth muscle cells. We hypothesized that *Bifidobacterium longum* NCC3001 metabolites alter the excitability of myenteric AH neurons in the ileum of the mouse. We quantified excitability by assessing a cell's threshold and electro-responsiveness. Electro-responsiveness is calculated as the number of action potentials elicited in response to a 500 ms supra-threshold depolarizing current injection (i.e., spike discharge) that was threshold plus 50 pA in intensity. Threshold refers to the intensity of current that is required to elicit one action potential (AP).

3.2 Methods

3.2.1 Longitudinal muscle-myenteric plexus preparation

All experiments were performed on sections of ileum excised from adult (6-8 week old) male (AKR; mice that express in all tissues the ecotropic retrovirus AKV) mice (The Jackson Laboratory, Bar Harbor, ME) immediately after the animal was sacrificed via cervical dislocation. The segments were placed in a recording dish on Sylgard® gel and opened along the

length of the mesenteric border and pinned flat under sufficient tension with insect pins with the mucosa facing upwards. During tissue preparation, the ileal segment was continuously submerged in Krebs solution (composition (in mM): NaCl (118.1), NaH_2PO_4 (1.0), $MgSO_4$ (1.2), $CaCl_2$ (2.5), KCl (4.8), glucose (11.1), $NaHCO_3$ (25)) and maintained at room temperature while constantly oxygenated with a gaseous mixture of 95% O_2-5% CO_2. 2 µM of nicardipine and 1 µM of scopolamine were added to the Krebs solution to prevent tissue contraction. Once the tissue was tautly pinned down, a longitudinal muscle myenteric plexus (LMMP) preparation was made using a pair of fine dissection forceps; the mucosa, submucosa, deep muscular plexus, and circular muscle layers were carefully removed to expose the myenteric plexus. The recording dish was then placed on the recording chamber of a high powered inverted microscope (Zeiss Axiovert S100 TV) and continuously perfused (4 mL/ min.) with Krebs solution at 37^{o}C.

3.2.2 Media preparation

Bifidobacterium longum NCC3001 was obtained from Nestlé Culture Collection (Lausanne, Switzerland) and cultured for 24 hours at 37°C under anaerobic conditions in de Man–Rogosa-Sharpe (MRS; unconditioned medium) broth containing 0.5% cysteine. The bacterial cells were separated by centrifugation for 15 minutes at 5000*g* at 4°C, resuspended again at a concentration of 10^{10} cells/ mL in their spent culture medium. Samples were kept in frozen (-80°C) aliquots until ready for use. The probiotic was prepared as previously described (Verdú et al., 2004). Before use, aliquots were filtered through a 0.2 µM filter to obtain bacteria-free conditioned medium (spent culture medium). Immediately before perfusion, a dilution was prepared containing 1 part of either the conditioned medium or the unconditioned medium (MRS

growth medium) to 20 parts of Krebs solution (containing 2 µM nicardipine and 1 µM scopolamine) under sterile conditions in a biological safety cabinet. This dilution was constantly oxygenated with a gaseous mixture of 95% O_2-5% CO_2 throughout the entire length of the experiment.

3.2.3 Electrophysiology

All preparations were allowed to equilibrate in Krebs solution for at least one hour prior to recording. Neurons were impaled with borosilicate glass micropipettes (fire polished; length: 7 cm; O.D: 1.5 mm; I.D: 0.86 mm) filled with 1 M KCl and fabricated to yield resistances between 100-120 MΩ. Recordings were made using a MultiClamp 700B amplifier (Axon Instruments). Signals were digitized at an acquisition rate of 500 kHz using a Digidata 1322A acquisition system (Axon Instruments) and stored on the PC.

After a neuron was impaled, action potential threshold of firing (rheobase) and resting membrane potential were determined with the injection of 500 ms depolarizing currents that were incrementally increased in intensity (step commands) until one action potential was fired at threshold. Immediately thereafter, action potential shape, action potential peak amplitude and duration at half width amplitude were determined with the injection of a 3-10 ms depolarizing current with an intensity of approximately threshold plus 100 pA. Thereafter, input resistance (R_{in}) and spike discharge were determined with the following protocol: a period of 500 ms of no current injection was followed by a 500 ms hyperpolarizing current injection with an intensity of -150 pA, followed by a 2 s period of no current injection, then followed by a 500 ms depolarizing current injection with an intensity of threshold plus 50 pA, which was proceeded by

a 6 second period of no current injection. This protocol was continuously repeated. During the last protocol is when the perfusate was changed from Krebs solution to either the conditioned or unconditioned medium. If at any point in this sequence of events the microelectrode were to dislodge and attempts to re-impale a cell were not successful, only those electrophysiological parameters which were measured were incorporated into the results. Ultimately, using these protocols, electrophysiological parameters were measured from an individual cell in one of the following settings: either in the presence of Krebs solution then again in the presence of one of the two media (conditioned or unconditioned), in the presence of the conditioned medium alone, or in the presence of the unconditioned medium alone.

3.2.4 Neurobiotin injection

The microelectrode used to record intracellular membrane potential changes was filled with 4 % Neurobiotin dye prior to experiment onset. At the end of the experiment, the following protocol was used to inject the Neurobiotin dye into the AH cell: injection of 500 ms current with threshold intensity (*as previously determined)*, repeating this injection once every second (total 30 injections). Immediately after this, the preparation was removed from the recording chamber of the microscope and fixed with Zamboni's fixative overnight where it was covered and placed in the fridge. The preparation was then washed with PBS-TX (PBS-triton X; 0.05 M with 0.3% TX-100, pH 7.4) 5 times for ten minutes each time. Next, the preparation was fixed in a solution containing 15 μL avidin-Texas Red: 3 mL PBS-TX and incubated for 90 minutes at 4^{o}C. The tissue preparation was then washed 3 times for ten minutes each time using the PBS-TX. After this, the tissue was ready for visualization, which was accomplished using an epi-

fluorescent microscope and then a confocal microscope was used to generate a high resolution figure.

3.2.5 Statistical Analysis

Data between conditioned and unconditioned media were compared using an unpaired Student's *t*-test. Statistical significance represents $p = 0.05$.

3.3 RESULTS

3.3.1 Identification of myenteric AH neurons in the mouse ileum

In accordance with previous studies involving the identification of myenteric neurons through conventional sharp electrode recording using a standard potassium chloride pipette solution (Mao et al., 2006), we identified intrinsic primary afferent neurons (AH neurons) using two criteria. A neuron was classified as an AH cell if it exhibited a broad action potential (half width duration between 1.8 ms and ~2.2 ms) with a hump on its falling phase (Clerc, Furness, Kunze, Thomas, & Bertrand, 1999). The hump was confirmed by the presence of an inflection in the first time derivative graph (dV/dT) of the voltage trace (Mao et al., 2006) (*lower case'* in Fig. 3.1 & 3.1). A neuron was also considered an AH cell by the presence of a slow after-hyperpolarization (sAHP) that was greater than 2 s in duration (Clerc, Furness, Bornstein, & Kunze, 1997; Clerc et al., 1999). Occasionally, an AH cell was filled with neurobiotin to reveal its multi-axonal morphology (Dogiel type II) (Fig. 3.3).

Fig. 3.1 Action potentials elicited in the presence of Krebs solution. *A*, A digital image of a ganglion in the myenteric plexus containing myenteric neurons, which are impaled using an intracellular microelectrode (*in white*). *B*, A neuron that fired four action potentials in response to a 500 ms current injection of 250 pA intensity in the presence of Krebs solution (n = 10). *b* & *b'*, Identification of calcium hump (*arrow*) with a time-derivative (dV/ dT) graph measured in the presence of Krebs solution. *C*, Graph depicting excitability (AP fired in response to a supra-threshold pulse) of neurons in the presence of Krebs solution (n = 10).

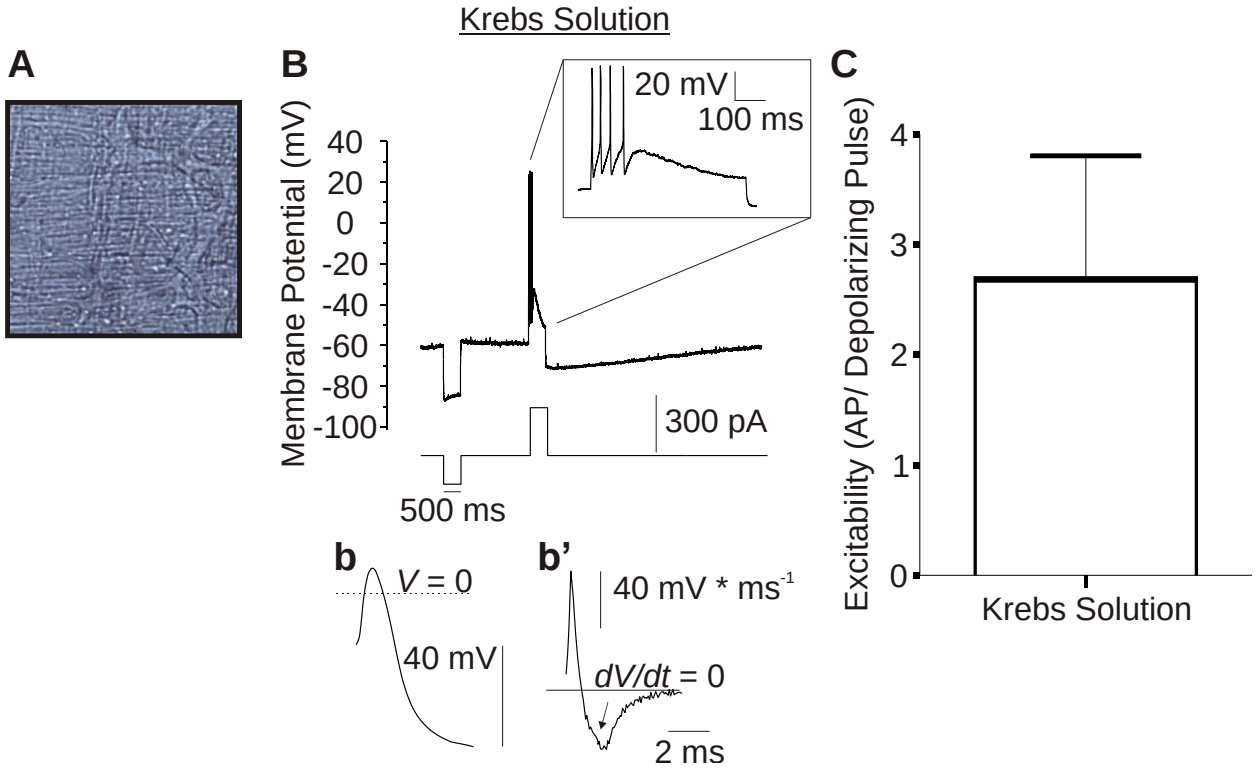
A
B
Krebs Solution
Membrane Potential (mV)
40
20
0
-20
-40
-60
-80
-100
20 mV
100 ms
300 pA
500 ms
b
V = 0
40 mV
b'
40 mV * ms-1
dV/dt = 0
2 ms
C
Excitability (AP/ Depolarizing Pulse)
4
3
2
1
0
Krebs Solution

Fig. 3.2 Excitability measured through spike discharge in myenteric AH neurons recorded using sharp microelectrodes filled with 1 M potassium chloride. Depolarizing and hyperpolarizing current injections had intensities equal to threshold plus 50 pA and -150 pA, respectively. *A* & *B*, Neurons that fired no action potentials in response to a 500 ms current injection of 450 pA and 350 pA intensity, respectively, in the presence of the conditioned medium (n = 5). In *a* & *a'*, Action potential configuration was measured in the presence of the conditioned medium using one protocol, which was followed by another protocol to assess spike discharge several minutes later in the same medium (*A*; voltage response). In *b* & *b'*, action potential configuration was measured in the presence of Krebs solution using one protocol, which was then followed by another protocol to assess spike discharge in the presence of the conditioned medium several minutes later (*B*; voltage response). *C* & *D*, Neurons that fired three and five action potentials in response to a 500 ms current injection of 400 pA and 250 pA intensity, respectively, in the presence of the unconditioned medium (n = 5). *Lower case* & *lower case'*, Identification of calcium hump (*arrow*) with a time-derivative (dV/ dT) graph.

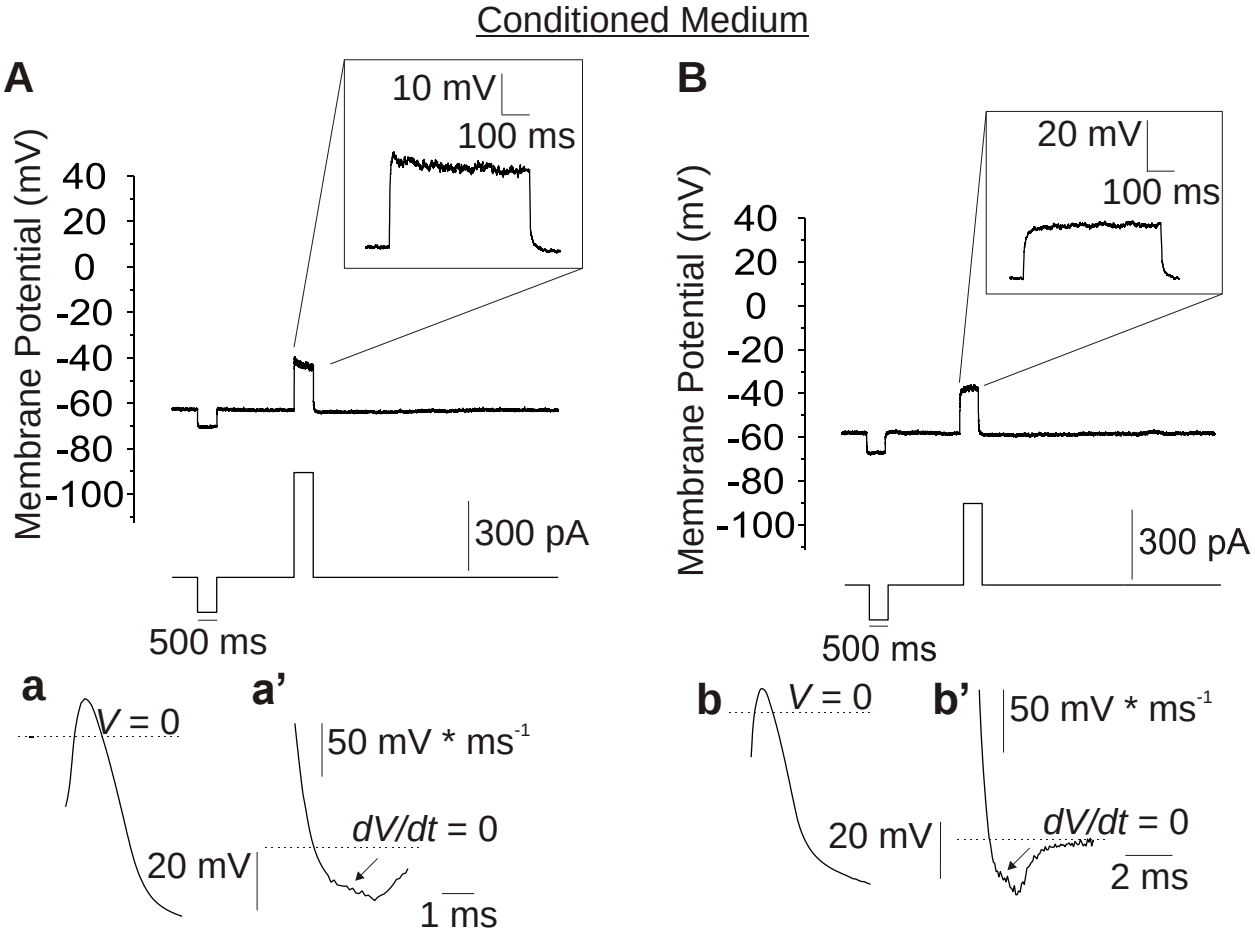
Conditioned Medium
A
10 mV
100 ms
Membrane Potential (mV)
40
20
0
-20
-40
-60
-80
-100
300 pA
500 ms
B
20 mV
100 ms
Membrane Potential (mV)
40
20
0
-20
-40
-60
-80
-100
300 pA
500 ms
a
V = 0
20 mV
a'
50 mV * ms-1
dV/dt = 0
1 ms
b
V = 0
20 mV
b'
50 mV * ms-1
dV/dt = 0
2 ms

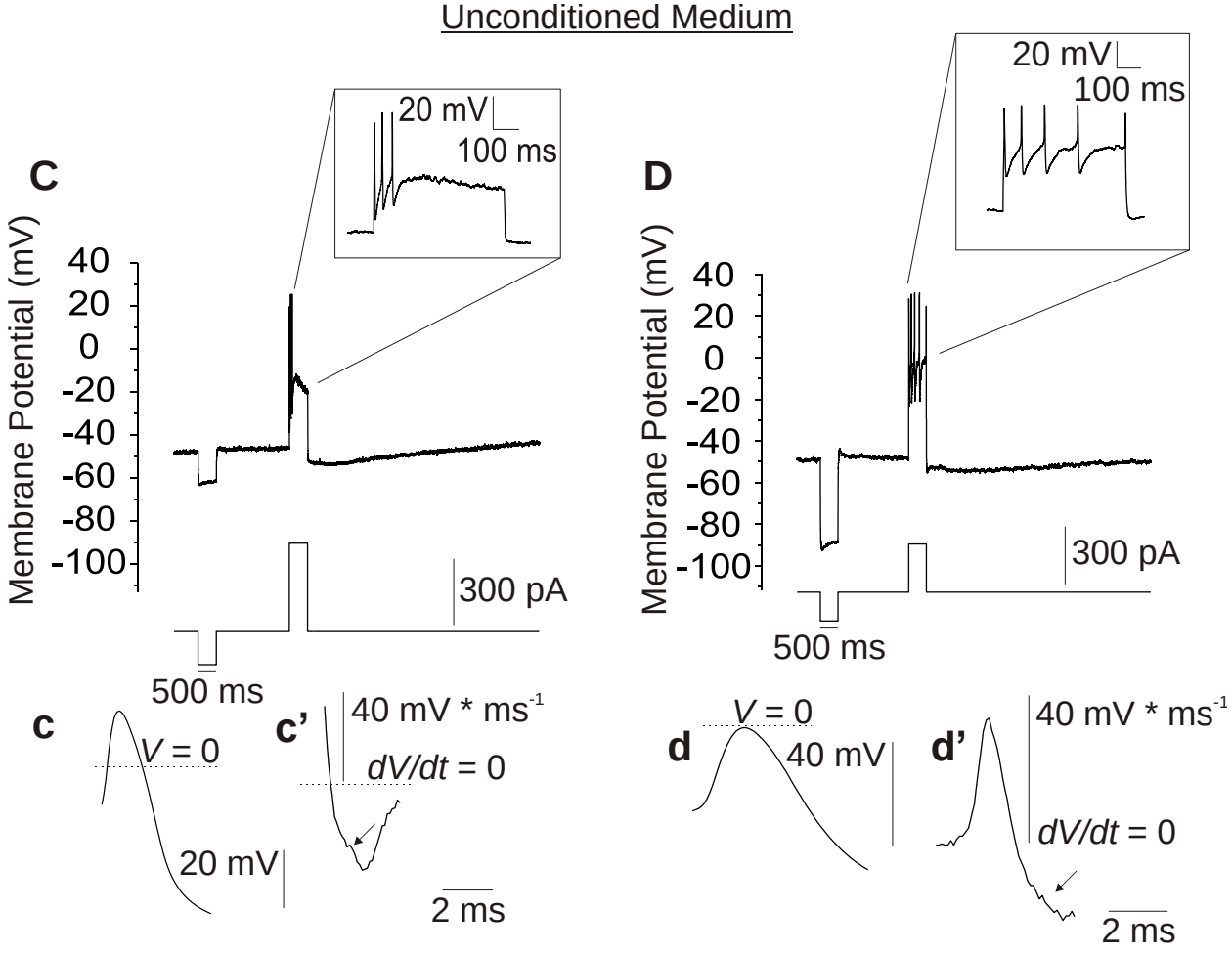
Unconditioned Medium
C
D
20 mV
100 ms
Membrane Potential (mV)
40
20
0
-20
-40
-60
-80
-100
300 pA
500 ms
c
c'
d
d'
V = 0
20 mV
40 mV * ms-1
dV/dt = 0
40 mV
2 ms

Fig. 3.3 Digital image of Texas Red fluorescence from an AH neuron that was injected with Neurobiotin dye to reveal its Dogiel type II morphology. Horizontal plane is the running direction of the circular muscle. Scale bar (*white line; bottom right corner)* indicates 20 μm. This image was obtained with the help of Dr. Yong Fang Zhu and Dr. Xuan-Yu Wang.

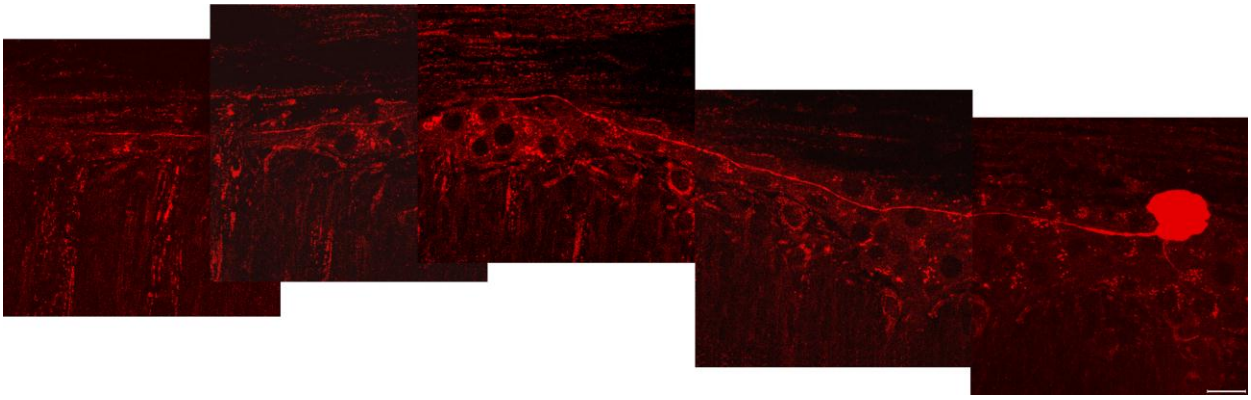

3.3.2 The effect of *Bifidobacterium longum* NCC3001 supernatant on the excitability of myenteric AH neurons in mouse ileum

We examined the effect of the perfusion of *Bifidobacterium longum* NCC3001 supernatant (conditioned medium) on AH neuron electro-responsiveness; with the perfusion of the MRS growth medium as control. Intracellular microelectrode recordings were performed on 47 myenteric neurons from 33 longitudinal muscle-myenteric plexus (LMMP) preparations. The electro-responsiveness as measured through spike discharge of AH cells perfused with the conditioned medium (n = 5) was significantly reduced compared to neurons perfused with the unconditioned medium (n = 5; P = 0.02; Fig. 3.2 & 3.4). Sensory neurons perfused with the conditioned medium (n = 9) exhibited a significant reduction in their instantaneous input resistances compared to neurons perfused with the unconditioned medium (n = 8; P = 0.01). There was also a significant reduction in the time-dependent input resistance of neurons perfused with the conditioned medium (n = 9) compared to neurons perfused with the unconditioned medium (n = 8; P = 0.02; Fig. 3.4). In addition, perfusion of the conditioned medium over sensory neurons (n = 9) significantly reduced the magnitude of the hyperpolarization-activated cationic current (I_h) compared to neurons perfused with the unconditioned medium (n = 8; P = 0.0003; Fig. 3.5). Furthermore, there was also a significant reduction in the action potential half width duration of myenteric sensory neurons perfused with conditioned medium (n = 5) compared to that exhibited by neurons perfused with the unconditioned medium (n = 5; P =

0.008). The electrophysiological properties of all recorded myenteric sensory neurons are summarized in Table 3.1.

Table 3.1: Electrophysiological properties of all recorded myenteric sensory neurons

	Krebs	**Conditioned Medium**	**Unconditioned Medium**
Membrane polarization (mV)	-57.8 ± 9.0 (n=28)	-56.0 ± 8.5 (n=14)	-59.9 ± 6.0 (n=8)
Rheobase (pA)	411.8 ± 203.4 (n=28)	300.0 ± 122.5 (n=9)	325.0 ± 119.0 (n=4)
AP peak amplitude (mV)	70.9 ± 9.9 (n=11)	59.4 ± 8.7 (n=5)	67.4 ± 11.1 (n=5)
AP half width duration (ms)	2.1 ± 0.4 (n=11)	1.9 ± 0.1 (n=5)	2.9 ± 0.6 (n=5)
Instantaneous Input Resistance (MΩ)	139.4 ± 93.7 (n=20)	70.2 ± 43.1 (n=9)	155.7 ± 78.9 (n=8)
Time-dependent Input Resistance (MΩ)	134.2 ± 87.6 (n=20)	69.7 ± 42.9 (n=9)	145.9 ± 75.2 (n=8)
Excitability (APs/ depolarizing pulse‡)	2.7 ± 3.5 (n=10)	0.2 ± 0.4 (n=5)	2.2 ± 1.4 (n=5)

Data is expressed as a mean ± S.D., with the numbers of observations in brackets.

‡ Depolarizing pulse is equal to rheobase plus 50 pA

mV: millivolts; pA: picoamperes; ms: millisecond; MΩ: Megohm

Fig. 3.4 Bar graphs depicting action potential thresholds, excitabilities, instantaneous input resistances, and time-dependent input resistances of neurons perfused with the conditioned and unconditioned media. *A*, No difference found between action potential thresholds of AH neurons perfused with the conditioned medium (n = 9) and those perfused with the unconditioned medium (n = 4; $P = 0.74$). *B*, Significant reduction in the excitabilities of AH neurons perfused with the conditioned medium (n = 5) as compared to those perfused with the unconditioned medium (n = 5; $P = 0.02$) when measuring spike discharge. Depolarizing pulses (†) were 50 pA plus the threshold in intensity (threshold determined in the presence of Krebs solution). *C*, There was a significant reduction in the instantaneous input resistance of neurons perfused with the conditioned medium (n = 9) as compared to those perfused with the unconditioned medium (n = 8, $P = 0.01$). *D*, There was also a significant reduction in the time-dependent input resistance of neurons perfused with the conditioned medium (n = 9) as compared to those perfused with the unconditioned medium (n = 8, $P = 0.02$).

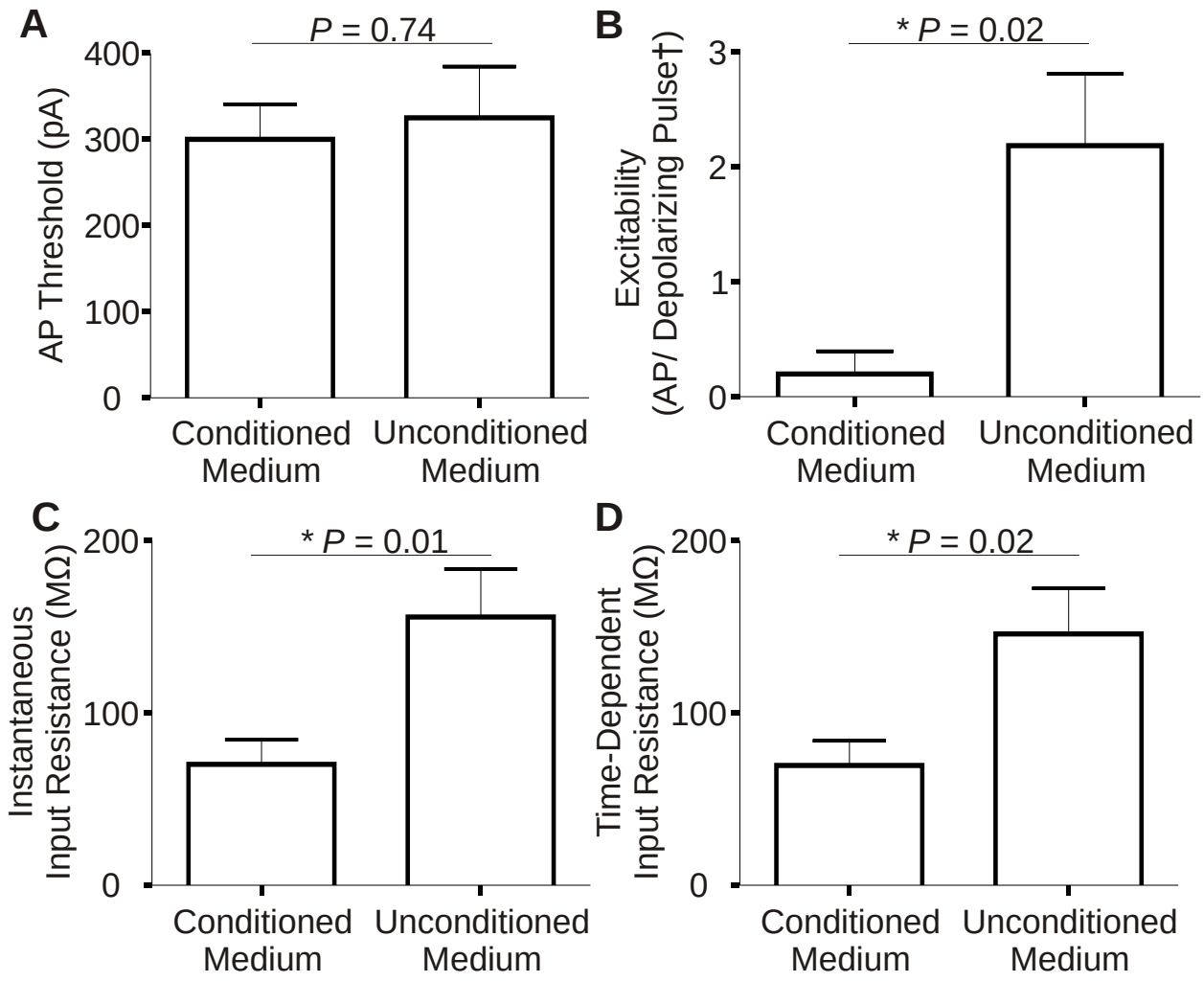
A
P = 0.74
AP Threshold (pA)
400
300
200
100
0
Conditioned Medium
Unconditioned Medium
B
* P = 0.02
Excitability (AP/ Depolarizing Pulse†)
3
2
1
0
Conditioned Medium
Unconditioned Medium
C
* P = 0.01
Instantaneous Input Resistance (MΩ)
200
100
0
Conditioned Medium
Unconditioned Medium
D
* P = 0.02
Time-Dependent Input Resistance (MΩ)
200
100
0
Conditioned Medium
Unconditioned Medium

Fig. 3.5 Contribution of a hyperpolarization-activated cationic conductance (I_h) to the excitability of myenteric AH neurons. *A,* The command current injection was a 500 ms hyperpolarizing current with -150 pA intensity (*lower panels*). In the presence of the unconditioned growth medium, this cationic current (I_h) is active (arrow) (n = 8). In the presence of *Bifidobacterium longum* NC 3001 supernatant (conditioned medium), this current is abolished (*upper panels*) (n = 9; * P = 0.0003). Time-dependent voltage values (‡) were subtracted from instantaneous voltage values (†) in order to quantify the slope or change in the I_h sag in the voltage recording over a 500 ms duration. The difference in input resistance between the beginning and the end of the hyperpolarizing pulse quantified I_h. *B,* Graph of I_h Δ values.

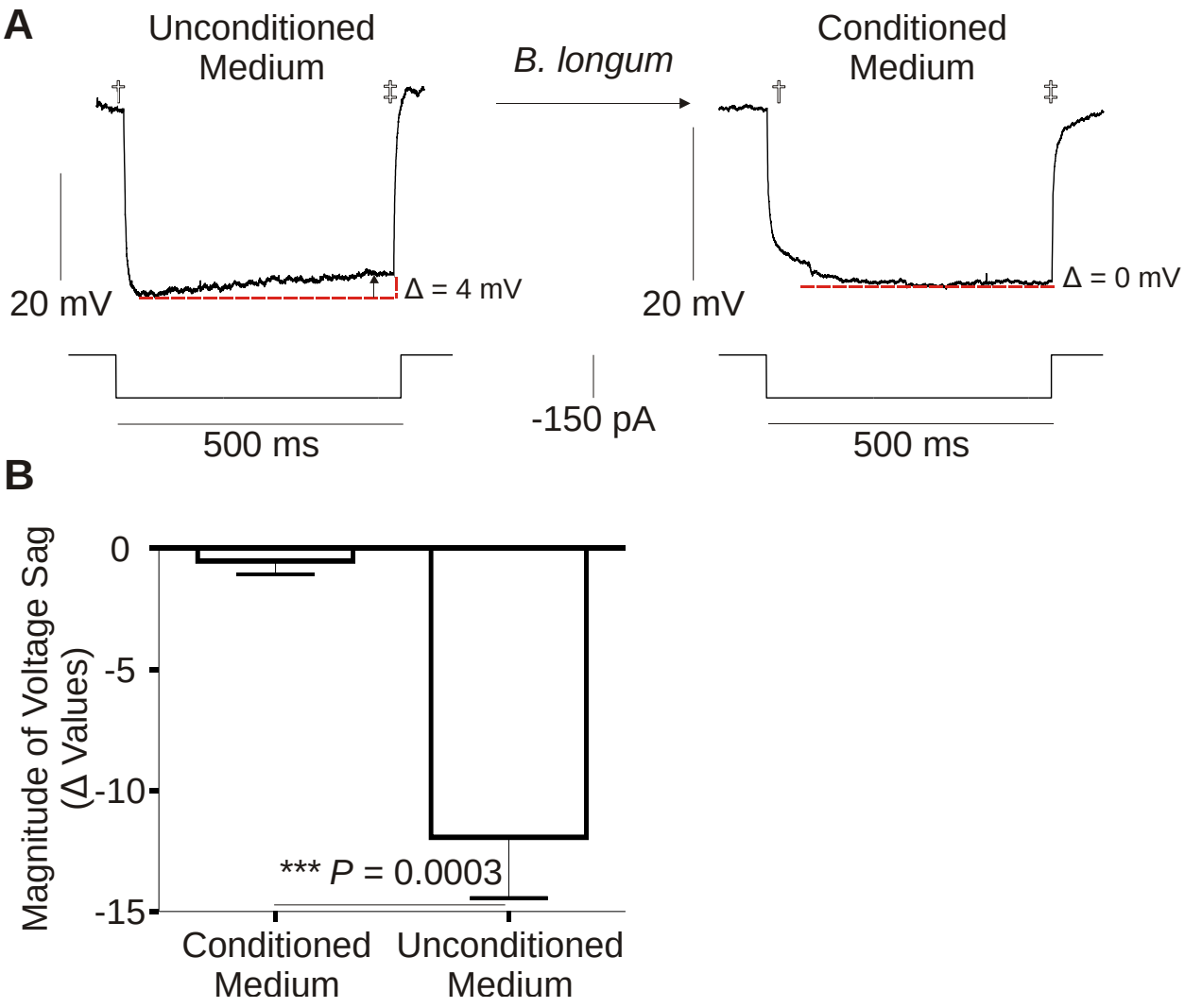
A
Unconditioned Medium
B. longum
Conditioned Medium
Δ = 4 mV
Δ = 0 mV
20 mV
20 mV
-150 pA
500 ms
500 ms
B
Magnitude of Voltage Sag (Δ Values)
0
-5
-10
-15
*** P = 0.0003
Conditioned Medium
Unconditioned Medium

3.4 Discussion

The present data indicate that *Bifidobacterium longum* NCC3001 supernatant decreases the excitability of myenteric AH neurons of the murine small intestine. This conclusion is supported by the fact that cells perfused with the conditioned medium exhibited a significant reduction in electro-responsiveness (*i.e*., spike discharge), input resistance, magnitude of their hyperpolarization-activated cationic conductance (I_h), and in their action potential durations at half width. Several electrophysiological parameters of AH neurons can be used as direct or indirect measures of excitability and in this present study we used spike discharge, input resistance, the magnitude of a hyperpolarization-activated cationic current (I_h), and action potential duration at half width as four criteria to conclude that the supernatant from this probiotic reduces the excitability of AH neurons. The neurons perfused with the conditioned medium displayed a significant reduction in input resistance, spike discharge, magnitude of their I_h, and action potential duration at half width. A reduction in input resistance means that more calcium-activated potassium channels are open allowing potassium to exit the cell and hyperpolarize it, which impedes the rate of firing in AH cells. A reduction in spike discharge means that at a given supra-threshold intensity current injection (*i.e.,* threshold plus 50 pA), the neuron fires fewer action potentials than neurons with higher rates of spike discharge. In order for an AH neuron to fire an action potential, its membrane potential must depolarize and reach the threshold of activation. Thresholds are a result of several cellular processes that determine the opening probabilities of different membrane channels, which individually contribute to the

whole conductance of a cell. A reduction in the I_h means that the HCN channels responsible for this conductance are closing or becoming inactivated and therefore not allowing cations such as sodium and calcium to enter and depolarize the cell. There was also a significant reduction in the duration of the action potentials at half amplitude in the conditioned group compared to that of neurons in the unconditioned group. A property unique to AH neurons is the calcium hump on the repolarizing phase of their action potentials, which is due to the conductance of an N-type calcium channel. The hump contributes to the duration of the action potential with larger humps typically giving rise to longer durations and; consequently, more calcium entering the cell. This calcium entry activates calcium activated potassium channels, which give rise to a potassium conductance that hyperpolarizes the cell and reduces excitability. This fact coupled with our results which show that cells perfused with the conditioned medium become less excitable and have lower resistances make it plausible that the supernatant from *B. longum* NCC3001 can evoke the opening of potassium channels. This explanation describes the fact that cells perfused with the conditioned medium have narrower action potentials but are less excitable.

It has long been known that a normal gut microbiota is required for the perseverance of normal motility patterns in animals (Abrams & Bishop, 1967; Caenepeel, Janssens, Vantrappen, Eyssen, & Coremans, 1989). Other studies have shown that probiotics such as *Lactobacillus reuteri* can decrease colorectal distension (CRD) – induced hyperexcitability of DRG neurons that projected into the colon, which were isolated and cultured after CRD (Ma et al., 2009). This moderation of pain transmission through probiotics was also shown in another study, which illustrated that *Lactobacillus paracasei* reduced antibiotic-induced visceral hypersensitivity to

CRD (Verdu et al., 2006). This probiotic has also been shown to attenuate muscle hypercontractility, which was associated with a reduction in a T-helper 2 response and a reduction in transforming growth factor-β1, cyclooxygenase-2, and prostaglandin E_2 levels in muscle (Verdú et al., 2004). Similar to this study, it was previously shown that *Lactobacillus reuteri* can also target IK_{ca} ion channels in enteric sensory neurons (W. A. Kunze et al., 2009). In a follow up study, it was elegantly shown that *Lactobacillus reuteri* can dose-dependently decrease jejunal motor complex pressure wave amplitudes in an *ex vivo* model (B. Wang, Mao et al., 2010). It was later shown that ingestion of this probiotic and IK_{ca} channel blockage both decrease rat colonic motility and propulsion (B. Wang, Mao, Diorio, Wang, Huizinga et al., 2010b). When interpreting the results of this study, it is important to keep in mind the gap that exists between these *in situ* experiments and a physiological setting. The composition of metabolites in the conditioned medium is relatively consistent because the conditions under which *Bifidobacterium longum* NCC3001 is cultured are well conserved; however, in a physiological setting results may vary. In culture, this probiotic has the potential to significantly proliferate without competition from other organisms, which allows *Bifidobacterium longum* NCC3001 to synthesize complex proteins and secondary metabolites if allowed to reach a stationary phase of growth. If this live *Bifidobacterium longum* NCC3001 is ingested and is able to colonize a normal gut where it will interact with the microflora population then it is plausible that the metabolites produced by this probiotic are different due to different growing conditions and the effect as seen on AH cells may change.

AH neurons are ‘sensory’ cells because they can be activated by chemical stimuli (W. A. Kunze et al., 2009; Wood & Mayer, 1978) or by process deformation and can be inhibited by mechanical distortion of their somas (W. A. A. Kunze et al., 2000). A unique attribute of AH neurons that make them distinct from S neurons is that only AH cells are chemosensory. In the present study, we show evidence that chemical stimuli from the metabolites of *Bifidobacterium longum* NCC3001 can have an effect on the action potential firing properties of an AH cell by reducing its excitability. Since these sensory cells are known to appose and form peristaltic reflexes with smooth muscles directly or indirectly through connections with interneurons and motor neurons (W. A. A. Kunze, Furness, & Bornstein, 1993), it seems logical to presume that *Bifidobacterium longum* can initiate changes in motility. In a recent study, it was shown that the integrity of the vagus nerve is required for the anxiolytic effects of *Bifidobacterium longum* NCC3001 during DSS-induced colitis. Since we known AH neurons can be stimulated by luminal products and can change motility patterns, it is likely that there is a means by which enteric neurons, such as AH cells, can communicate with the central nervous system (CNS).

Recently in a fascinating study, it was shown that the terminal fields of vagal mechanoreceptors called intramuscular arrays (IMAs) that innervate the rat gastric smooth muscle are connected to nodose ganglia using a neuroanatomical tracer. Double labeling interstitial cells of Cajal (ICC) with c-Kit and neuron fibers with CGRP (calcitonin-gene related peptide) stain revealed that these IMAs make extensive contacts with ICC where CGRP+ fibers also intermingle (Powley & Phillips, 2011). These CGRP+ fibers can potentially be AH cells and may provide a possible route whereby sensory afferents can communicate with vagal neurons

and subsequently communicate with the brain stem. In this manner, luminal challenges can be monitored by the CNS and enteric neurons act as gateways between the lumen and the CNS. Whether the CNS receives notice of this change in motility through changes in smooth muscle contractility (monitored by CNS via vagus) or through changes in the properties of AH cells directly requires further investigation.

The effects of the conditioned medium on myenteric AH cells occurs relatively fast (few minutes), which suggests the effect to be directly on enteric neurons; however, the possibility that the effects of the conditioned medium may be mediated through endocrine cells or immune cells is not eliminated. Enterochromaffin cells (EC cells) are a population of enteroendocrine cells that are located in the epithelium of the digestive tract and produce more than 95% of total intestinal 5-HT (serotonin) content (Racke, Reimann, Schwörer, & Kilbinger, 1995). EC cells can be stimulated by luminal content such as sugars (Y. Li, Hao, Zhu, & Owyang, 2000) and by mechanical distortion (A. Kirchgessner, Tamir, & Gershon, 1992; Y. Li et al., 2000) and subsequently release serotonin, which can reach the receptors on AH cells, which include 5-HT_3, 5-HT_4, and 5-HT_{1P} (Furness, 2006). EC cells are in close proximity to lymphocytes in the gut wall in the digestive tract and are therefore able to activate immune cells and elicit immune responses, which can ultimately have an effect on AH cells and the surrounding gut musculature (Kidd, Gustafsson, Drozdov, & Modlin, 2009). Furthermore, dendritic cells (DC) found in intact gut wall are antigen presenting cells that can actually engulf and capture bacterial products (such as LPS) and transport them to lymphoid tissue where they can induce the activation of naïve T

cells and thus an immune response (Stagg, Hart, Knight, & Kamm, 2003), which can cause inflammation of the digestive tract and plausibly affect AH cells and gut musculature.

CHAPTER 4.0: EFFECT OF *BIFIDOBACTERIUM LONGUM* NCC3001 ON SLOW WAVE ACTIVITY OF THE MOUSE INTESTINE

PREFACE

The results from our study of the effects of *Bifidobacterium longum* NCC3001 supernatant intrigued us to investigate the action of the supernatant on the musculature of the gut. Many studies focus on the effects of probiotics on enteric nerves and some focus on musculature; however, seldom do we find a study that investigates the effects of a probiotic or commensal on both the enteric nerves and musculature of the gastrointestinal tract. This approach is ideal in developing a comprehensive understanding of the effects and mechanisms of action of a probiotic.

4.1 Introduction

Early studies postulated that the slow wave of the small intestine is associated with the spontaneous generation of the pacemaker interstitial cells of Cajal of the myenteric plexus (ICC-MP) (Holaday, Volk, & Mandell, 1958). We now know that this is true because the slow wave is only generated when there is an intact network of ICC-MP (Huizinga et al., 1995; Nakagawa et al., 2005). Without this network of interstitial cells of Cajal, there would be no peristaltic waves to propagate from the oral to the anal end (Nakagawa et al., 2005). Also, it is recognized that the

pacemaker potential is a rhythmic oscillation of the membrane potential of ICC-MP and that the slow wave is coupled to this as rhythmic oscillation of membrane potential in the smooth muscle, which is generated through an electrotonic spread of pace maker potentials (Kito & Suzuki, 2003). In order for the small intestine to propel luminal content, the propagating slow waves need to be superimposed by action potentials generated by the smooth muscle cells (Huizinga, Ambrous, & Der-Silaphet, 1998a). Furthermore, there have been studies that have illustrated that the small intestine is capable of generating two electrical patterns (Diamant & Bortoff, 1969; Huizinga, Ambrous, & Der-Silaphet, 1998a). Together, these two oscillating patterns of the membrane potential appear to have a waxing and waning configuration. Previously, it has been shown that the frequency of slow waves decreases aborally and that there are periods of waxing and waning separated by *frequency plateaus* in different positions along the length of an intact small intestine (Diamant & Bortoff, 1969). It was hypothesized that in a frequency plateau, a dominant oscillator with the highest intrinsic frequency drives oscillation patterns, whereas in areas of waxing and waning either the coupling between oscillators in insufficient or the frequency of oscillators are not synchronized because the frequency of a driving oscillator is too high.

We attempt to measure membrane potentials experienced by circular smooth muscles that illustrate the two previously described electrical patterns. Our goal is to gain a better understanding of the mechanisms involved in generating these electrical patterns by mimicking

neurotransmission to the smooth muscle cells through the use of exogenous carbachol and L-NNA and by administering the conditioned medium of *Bifidobacterium longum* NCC3001.

4.2 Methods

4.2.1 Tissue preparation

All experiments were performed on sections of proximal small intestine excised from adult male AKR mice (The Jackson Laboratory, Bar Harbor, ME) (6-8 week old) or neonatal male CD1 mice (Charles River Laboratories International, Inc., Wilmington, MA) immediately after the animal was sacrificed via cervical dislocation. The segments were placed in a recording dish on Sylgard® gel and opened along the length of the mesenteric border and pinned flat under low tension with insect pins with the mucosa facing upwards. During tissue preparation, the tissue segment was continuously submerged in Krebs solution (composition (in mM): NaCl (118.1), NaH_2PO_4 (1.0), $MgSO_4$ (1.2), $CaCl_2$ (2.5), KCl (4.8), glucose (11.1), $NaHCO_3$ (25)) and maintained at room temperature while constantly oxygenated with a gaseous mixture of 95% O_2-5% CO_2. Once the tissue was pinned down, the mucosa and submucosa were carefully removed using a pair of fine dissection forceps to expose the circular smooth muscle layer. The recording dish was then placed on the recording chamber of a high powered inverted microscope (Zeiss Axiovert S100 TV) and continuously perfused (4 mL/ min.) with Krebs solution at 37^{o}C.

4.2.2 Media preparation

Bifidobacterium longum NCC3001 was obtained from Nestlé Culture Collection (Lausanne, Switzerland) and cultured for 24 hours at 37°C under anaerobic conditions in de

Man–Rogosa-Sharpe (MRS; unconditioned medium) broth containing 0.5% cysteine. The bacterial cells were separated by centrifugation for 15 minutes at 5000*g* at 4°C, resuspended again at a concentration of 10^{10} cells/ mL in their spent culture medium. Samples were kept in frozen (-80°C) aliquots until ready for use. The probiotic was prepared as previously described (Verdú et al., 2004). Before use, aliquots were filtered through a 0.2 μM filter to obtain bacteria-free conditioned medium (supernatant).

A dilution was then prepared containing Krebs solution and either the conditioned medium or unconditioned medium in a 20:1 ratio, respectively, under sterile conditions in a biological safety cabinet, oxygenated with a gaseous mixture of 95% O_2-5% CO_2 throughout the entire length of the experiment.

4.2.3 Electrophysiology

All preparations were allowed to equilibrate in Krebs solution for at least one hour prior to recording. Circular smooth muscle cells were impaled with borosilicate glass micropipettes (fire polished; length: 7 cm; O.D: 1.5 mm; I.D: 0.86 mm) filled with 3 M KCl and fabricated to yield resistances between 50-70 MΩ. Recordings were made using a MultiClamp 700B amplifier (Axon Instruments). Signals were digitized at an acquisition rate of 500 kHz using a Digidata 1322A acquisition system (Axon Instruments) and stored on the PC.

A direct current was used with zero intensity and used to record membrane potentials experienced by the cell near the level of the deep muscular plexus.

4.2.3 Statistical analysis

Data between groups were compared using a paired Student's *t*-test. Statistical significance represents $p = 0.05$.

4.3 Results

4.3.1 Slow wave activity of the mouse proximal small intestine

We recorded the electrical slow wave of circular smooth muscles at the level of the deep muscular plexus. We always observed and recorded the normal pacemaker slow wave pattern associated with spontaneously generating ICC-MP (interstitial cells of Cajal in the myenteric plexus) (Fig 4.1) but would often observe a second slower pattern of frequency (1 cycle every ~30 seconds) from unidentified origins. These two patterns were observed in the proximal small intestine of adult mice during the perfusion of Krebs solution (Fig. 4.2).

With consideration that ICC-DMP (interstitial cells of Cajal in the deep muscular plexus) may potentially interact with the circular smooth muscle layer, we used neonatal mice in a subset of preliminary experiments in efforts to preserve this network. Using the exact same protocols as for the adult preparations, we also observed the two patterns of frequency in neonatal preparations but with no advantage over adult animals in terms of number of observations (Fig. 4.3).

4.3.2 The effect of exogenous carbachol and L-NNA on the slow wave activity of the mouse proximal small intestine

We wanted to mimic the role of neurotransmission and study its effects on these two patterns of frequency. Prior to the addition of 1μM carbachol (Fig. 4.4A) or $2e^{-4}$ M L-NNA (Nitroarginine; competitive inhibitor of nitric oxide synthase; Fig. 4.5A), we would only observe

the pacemaker slow wave during the perfusion of Krebs solution. Upon the addition of carbachol (n = 3; Fig. 4.4B) or L-NNA (n = 4; Fig. 4.5B), we would observe this second slower frequency pattern appear. The resting membrane potentials (RMPs) of smooth muscle cells in the presence of 1μM carbachol were significantly depolarized relative to the resting membrane potential of those cells in the presence of Krebs solution (n = 7; P = 0.05; Table 4.1). Other than this difference, there were no differences in any characteristics of the slow wave between cells perfused with the Krebs solution and those perfused with either carbachol or L-NNA.

Fig. 4.1 Pacemaker slow wave recorded from circular smooth muscle of the jejunum in adult mouse. Normal slow wave activity recorded from the circular smooth muscle from a tissue segment from the jejunum of the small intestine using a borosilicate microelectrode filled with 3M KCl with a resistance of 50 MΩ. Individual waves have a rapid upstroke followed by a plateau phase. Slow wave oscillations in this preparation had a frequency of 29 cycles per minute with cycle duration of approximately 2 s. The resting membrane potential of this cell was -67 mV. This tissue was under minimal tension.

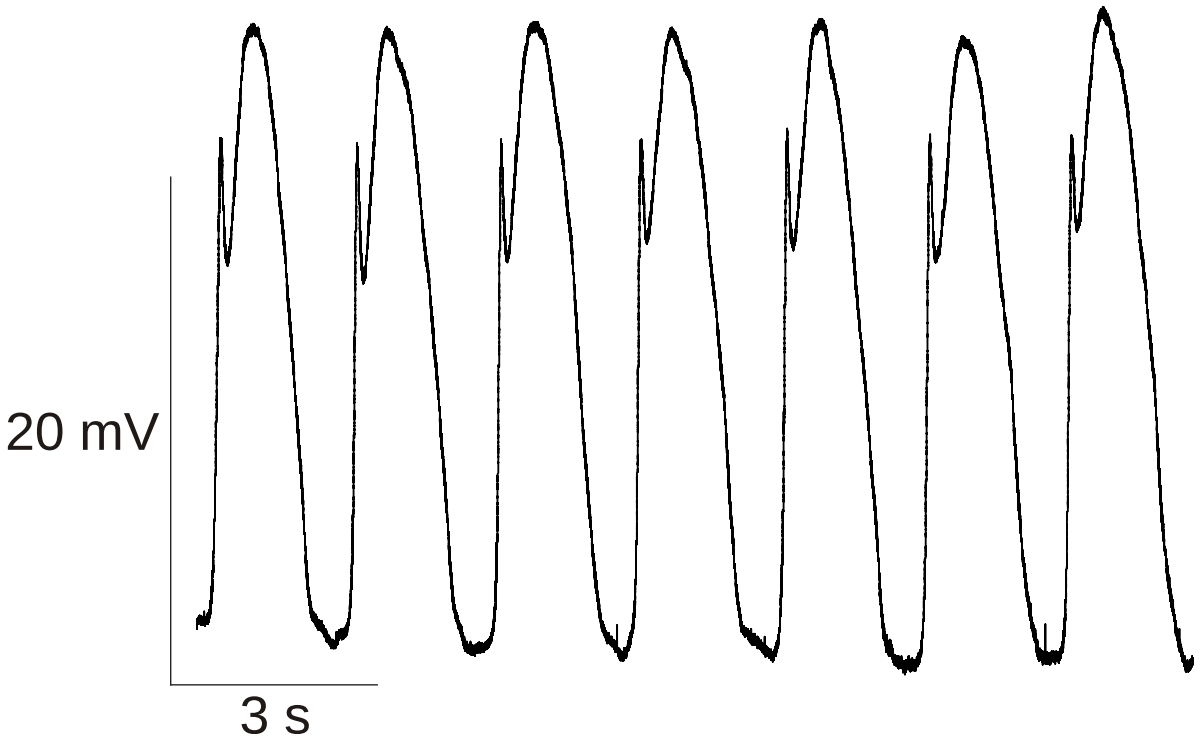
20 mV
3 s

Fig. 4.2 Two patterns of frequency measured in the circular smooth muscle of the adult mouse jejunum during the perfusion of Krebs solution using an intracellular microelectrode. Two patterns of frequency recorded from the circular smooth muscle from a tissue segment from the duodenum-jejunum region of the small intestine using a borosilicate microelectrode filled with 3 M KCl with a resistance of 50 MΩ. One pattern is the high frequency slow wave associated with the interstitial cells of Cajal in the myenteric plexus, with a frequency of 20-30 cycles per minute. The second slower frequency pattern occurs, on average, once every 36 s. The resting membrane potential of this cell was -43 mV. This tissue was under minimal tension.

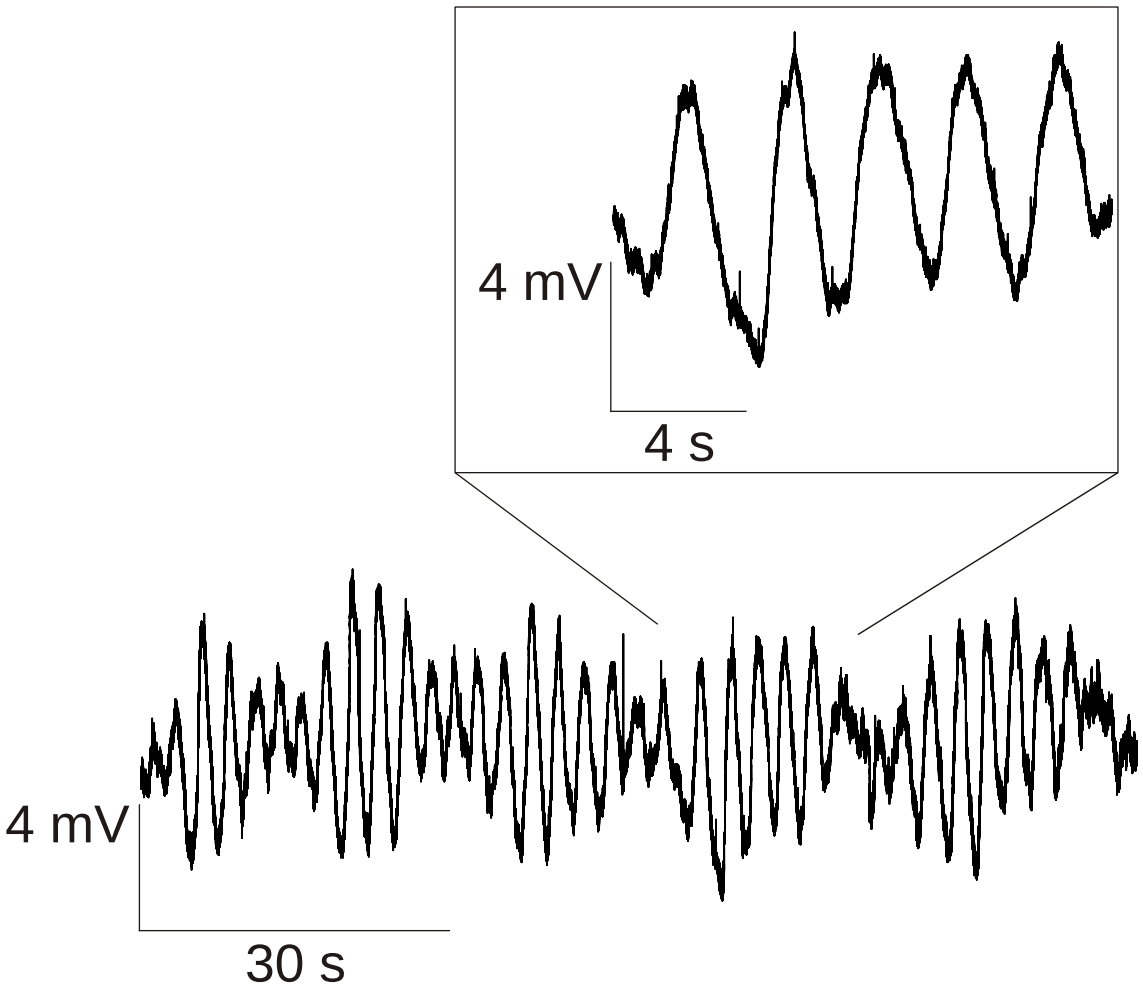
4 mV
4 s
4 mV
30 s

Fig. 4.3 Two patterns of frequency measured in the circular smooth muscle of the neonatal mouse jejunum during the perfusion of Krebs solution using an intracellular microelectrode. Two patterns of frequency recorded from the circular smooth muscle from a tissue segment from the duodenum-jejunum region of the small intestine using a borosilicate microelectrode filled with 3 M KCl with a resistance of 50 MΩ. One pattern is the high frequency slow wave associated with the interstitial cells of Cajal in the myenteric plexus, with a frequency of 20-30 cycles per minute. The second slower frequency pattern occurs, on average, once every 36 s. The resting membrane potential of this cell was -46 mV. This tissue was under minimal tension.

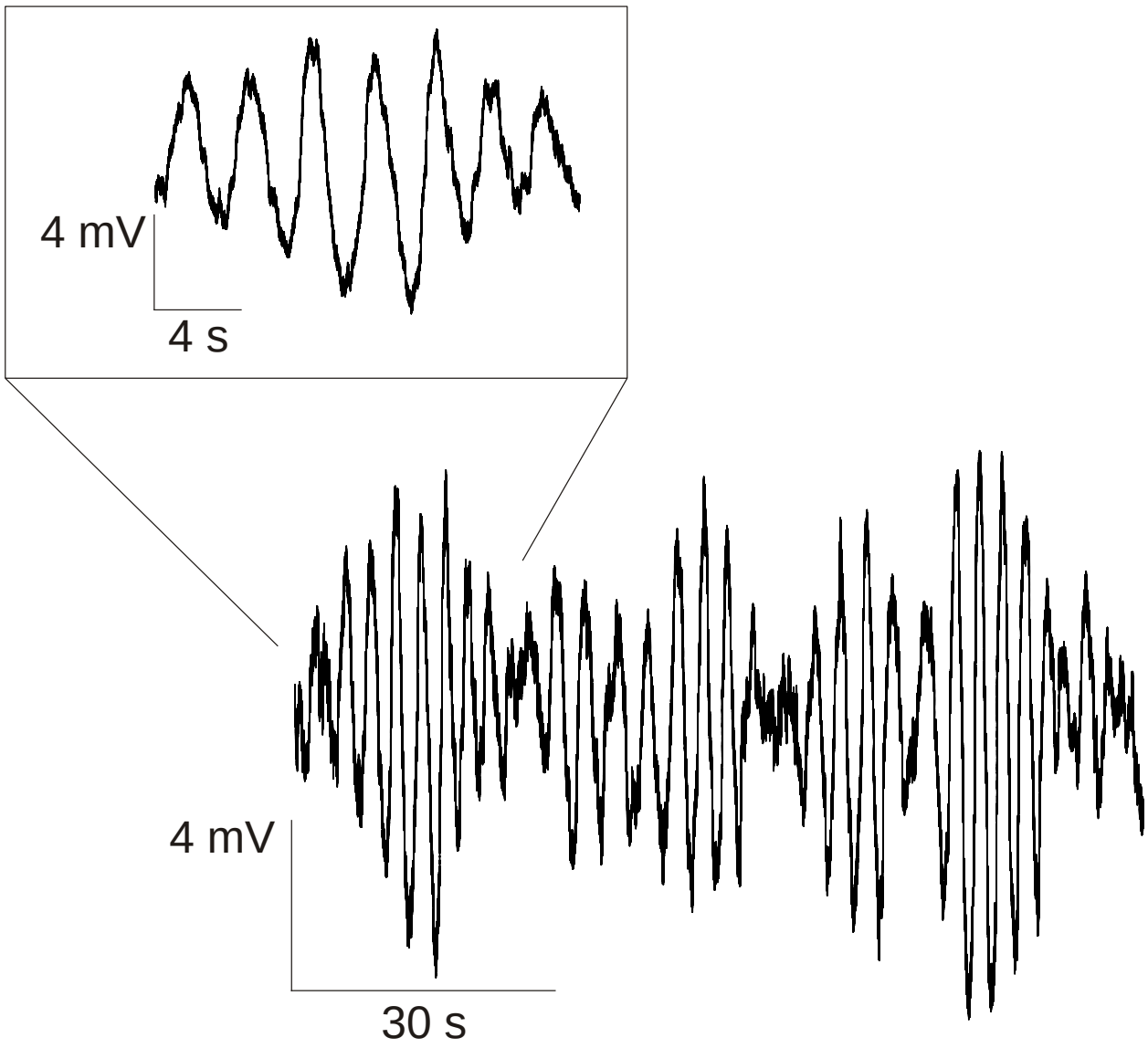
4 mV
4 s
4 mV
30 s

Fig. 4.4 The effect of 1μM carbachol on the two patterns of frequency measured from the circular smooth muscle of the jejunum of an adult mouse. *A*, Only the high frequency slow wave associated with the interstitial cells of Cajal in the myenteric plexus (30 cycles/min.) visible during the perfusion of Krebs solution. *B*, The addition of 1μM carbachol to the perfusate (Krebs) induced a second frequency to appear (approx. 1 cycle/ 25 s) (n = 3). The resting membrane potential of this cell before and after the addition of carbachol was -57 mV and -52 mV, respectively. This tissue was under minimal tension.

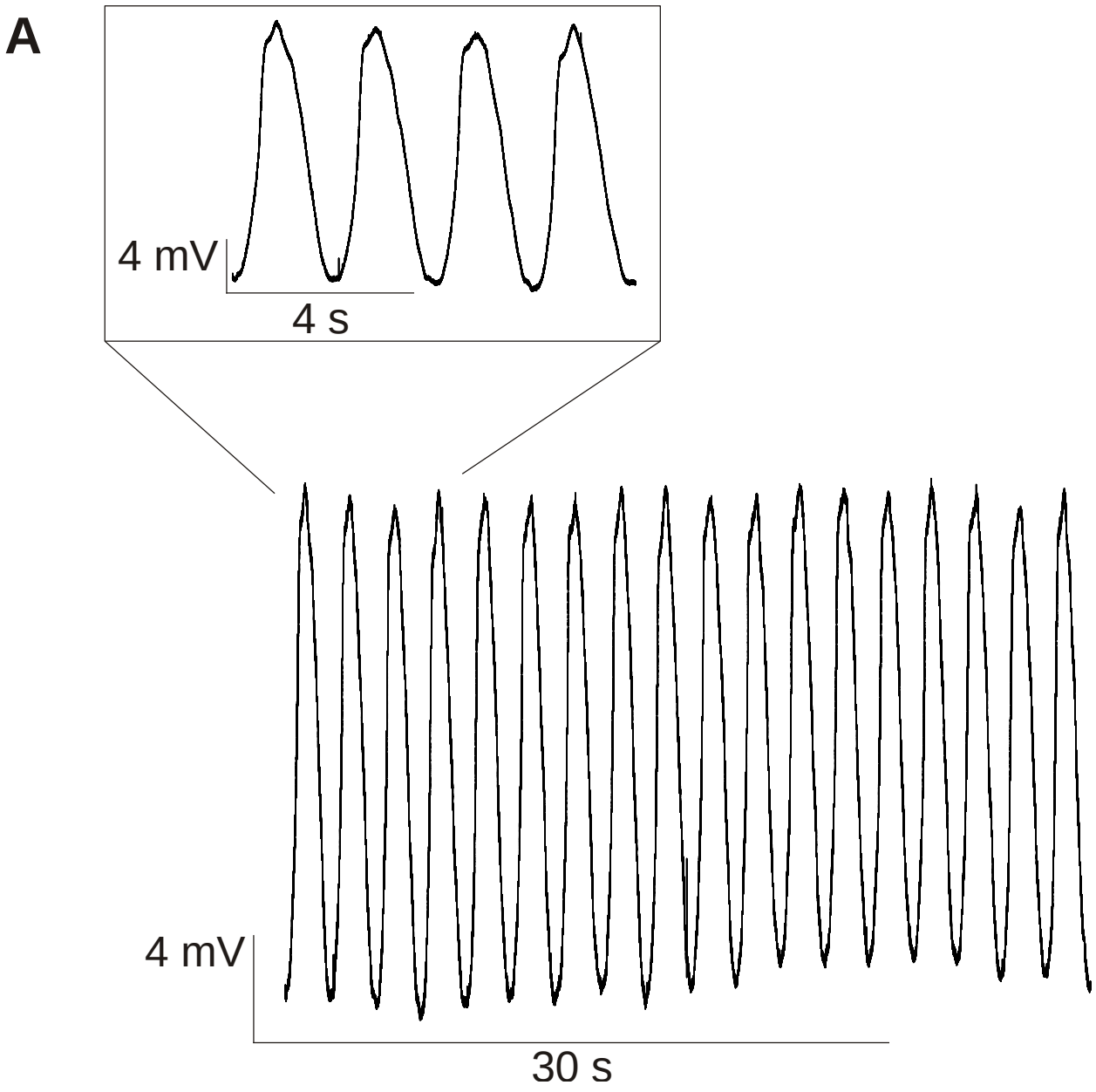
A
4 mV
4 s
4 mV
30 s

B

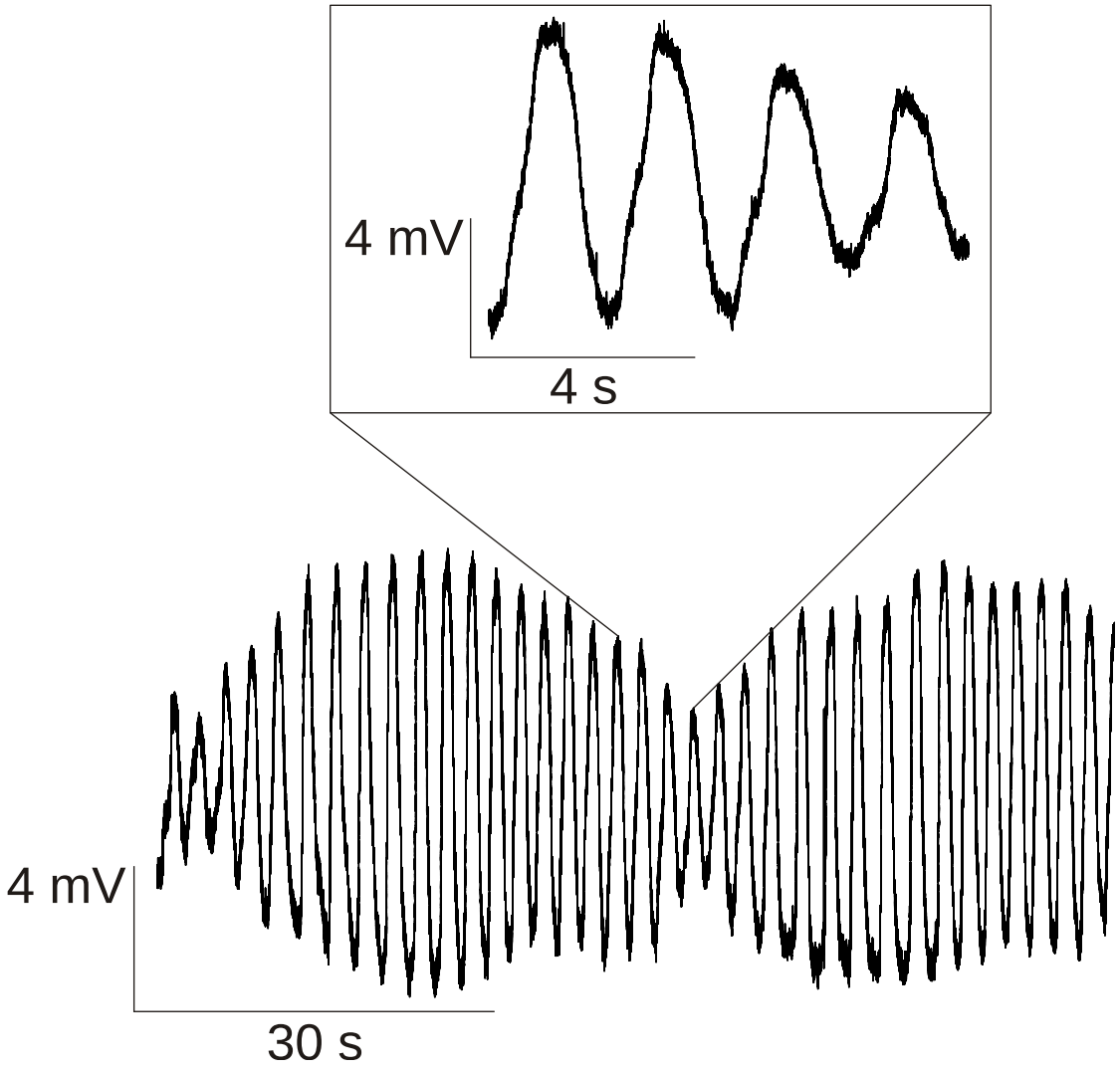

Fig. 4.5 The effect of $2e^{-4}$ M L-NNA on the two patterns of frequency measured from the circular smooth muscle of the jejunum of an adult mouse. *A*, Only the high frequency slow wave associated with the interstitial cells of Cajal in the myenteric plexus (24 cycles/min.) visible during the perfusion of Krebs solution. *B*, The addition of $2e^{-4}$ M L-NNA to the perfusate (Krebs) induced a second frequency to appear (approx. 1 cycle/ 28 s) (n = 4). The resting membrane potential of this cell before and after the addition of L-NNA was -73 mV and -67 mV, respectively. This tissue was under minimal tension.

A

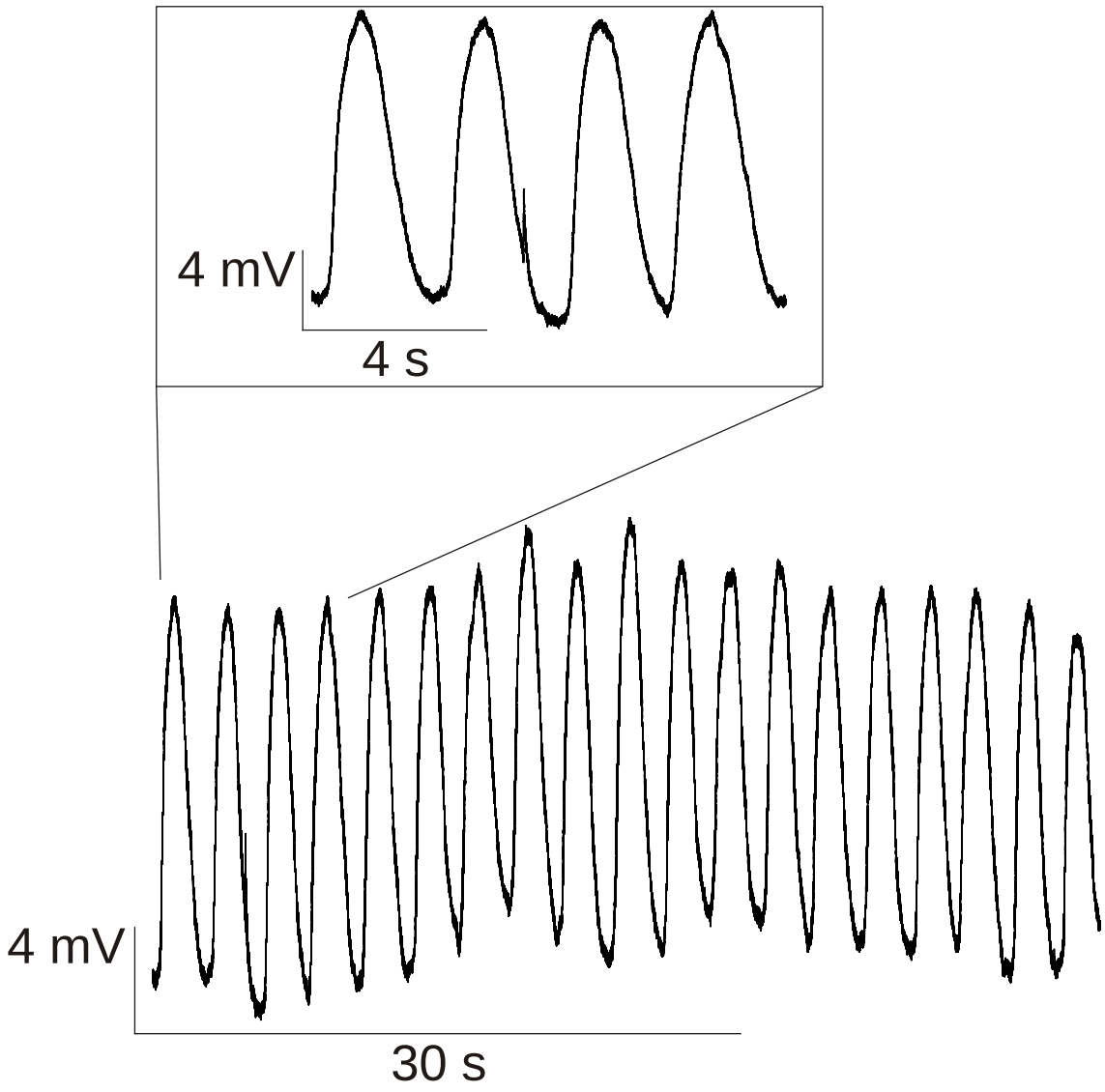

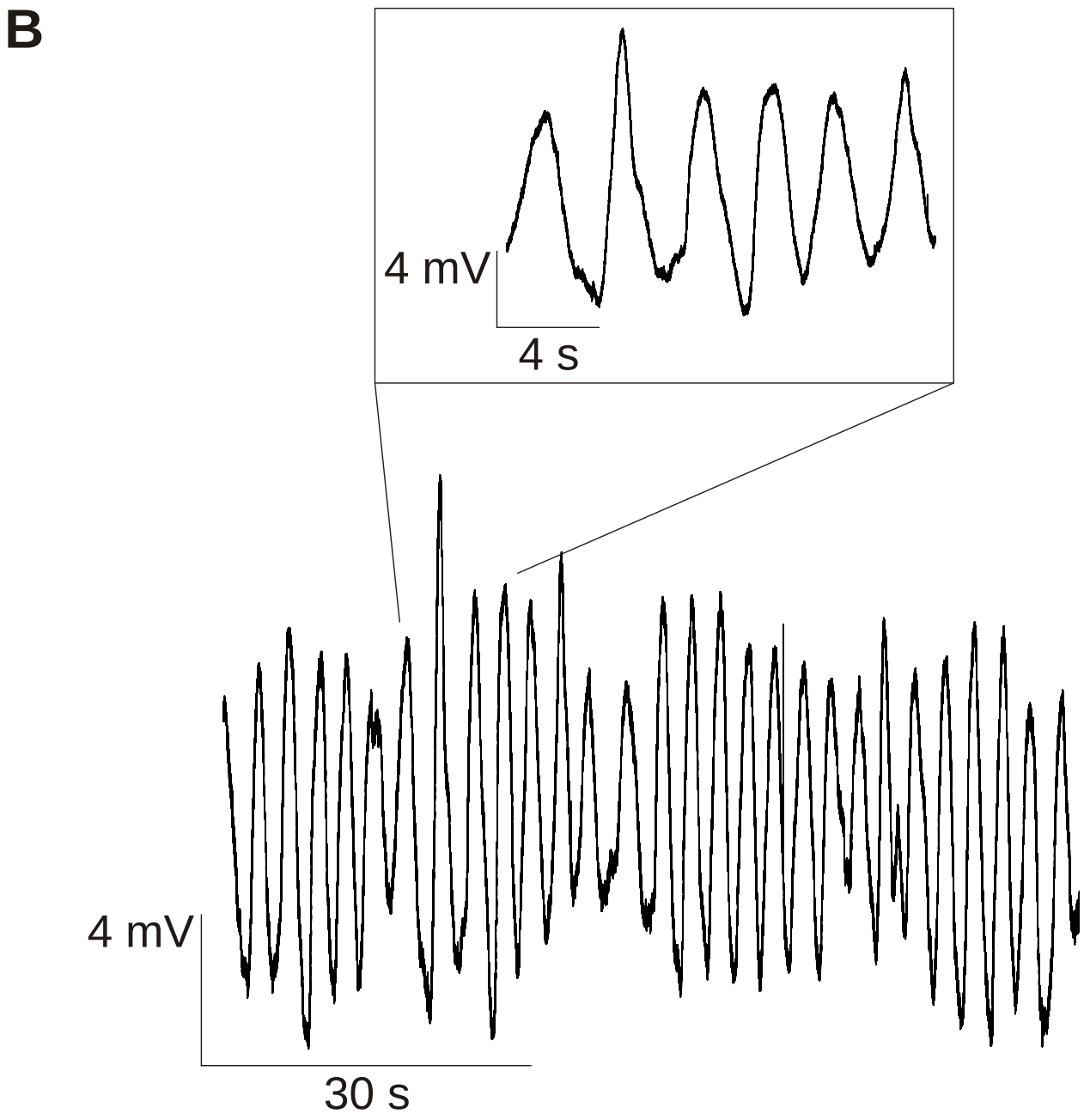
B
4 mV
4 s
4 mV
30 s

4.3.3 The effect of *Bifidobacterium longum* NCC3001 supernatant on the slow wave activity of the mouse proximal small intestine

Upon full immersion, the supernatant of *Bifidobacterium longum* NCC3001 (conditioned medium) caused an initial depolarization of the circular smooth muscle cell. This depolarization continued until the slow wave oscillations in these cells ceased and membrane potential would plateau (Fig. 4.6A). Shortly after this plateau, the slow wave oscillations reappeared and the cell was hyperpolarized (Fig. 4.6B). Data were collected only when a stable recording could be achieved, which was during the perfusion of Krebs solution and after the addition of the conditioned medium when the cell subsequently hyperpolarized after a state of initial depolarization (Table 4.1). No data were collected during the plateau phase of the effect since the slow wave was abolished in these periods. The resting membrane potential of circular smooth muscle cells in Krebs solution was -54.3 mV and -70.3 mV approximately two minutes after full immersion by the supernatant when the cell was hyperpolarized and a stable recorded was achieved (n = 7; P = 0.02; Table 4.1). The average time of onset of depolarization was 18.6 s and the average absolute change in membrane potential from onset of effect to its plateau (depolarization) was 16.0 mV (n = 7). Occasionally, the addition of the conditioned medium only caused an immediate but slight depolarization (n = 3) and in other cases caused only a hyperpolarization of the cell (n = 3) with no significant changes in the measured parameters of the cell in either case (Table 4.1). Furthermore, any cells that exhibited the waxing and waning of the slow wave lost this pattern upon the addition of the conditioned medium (n = 10; Table 4.1).

Fig. 4.6 The effect of *Bifidobacterium longum* NCC3001 supernatant on the slow wave activity of the circular smooth muscle of the jejunum of an adult mouse. *A,* Only the high frequency slow wave associated with the interstitial cells of Cajal in the myenteric plexus are visible during the perfusion of Krebs solution with a frequency of 29 cycles/minute. The addition of the conditioned medium (*arrow*) caused an initial depolarization of the membrane potential until it reached a plateau phase. The resting membrane potential of this cell before the addition of the conditioned medium (*arrow*) was -55 mV. *B,* Approximately two minutes after the initial depolarization and plateau, the resting membrane potential of the cell was relatively hyperpolarized and the slow waves appeared with characteristics similar to those prior to the addition of the conditioned medium. The resting membrane potential of the cell remained at -67 mV thereafter. This tissue was under minimal tension.

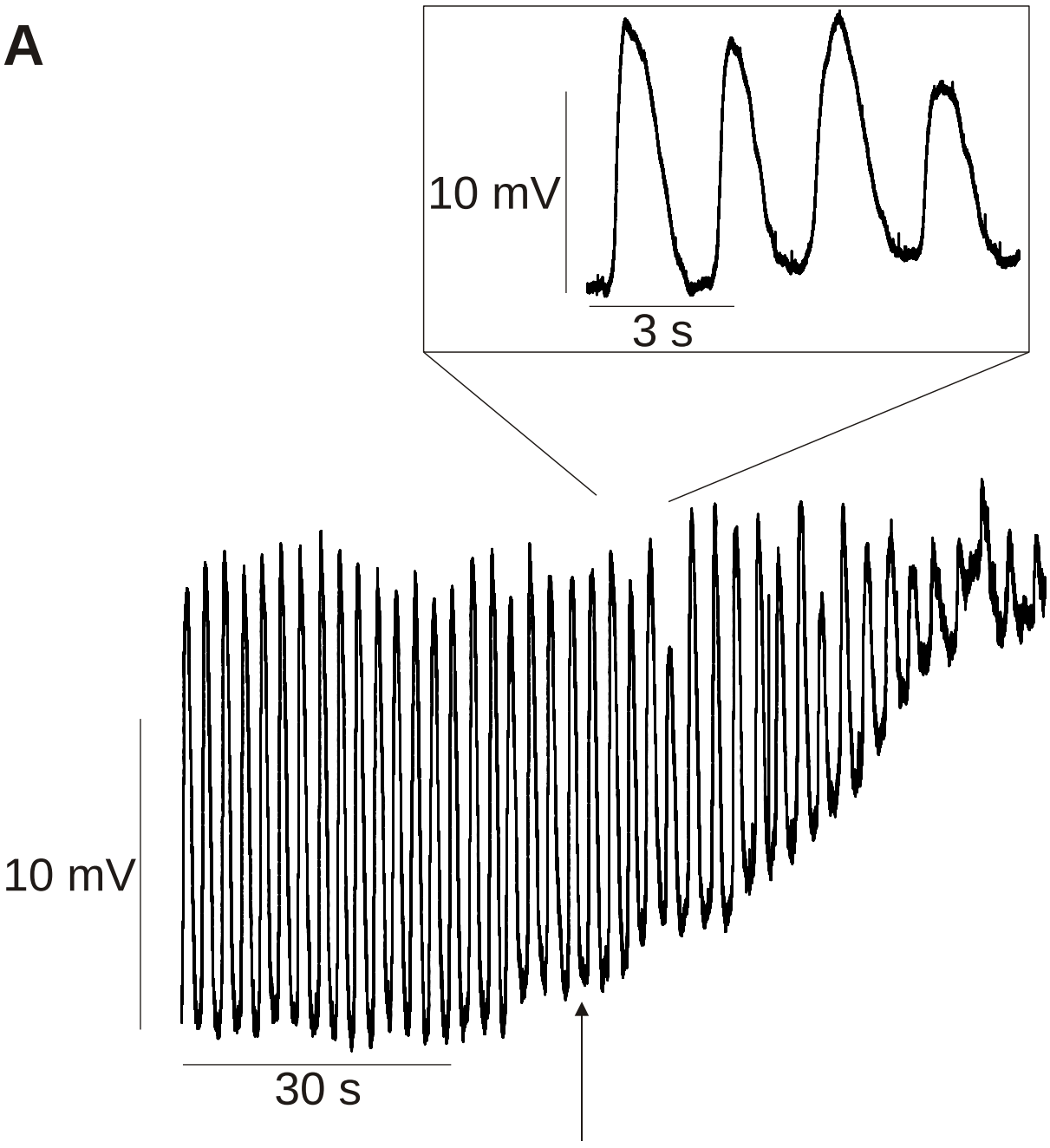
A
10 mV
3 s
10 mV
30 s

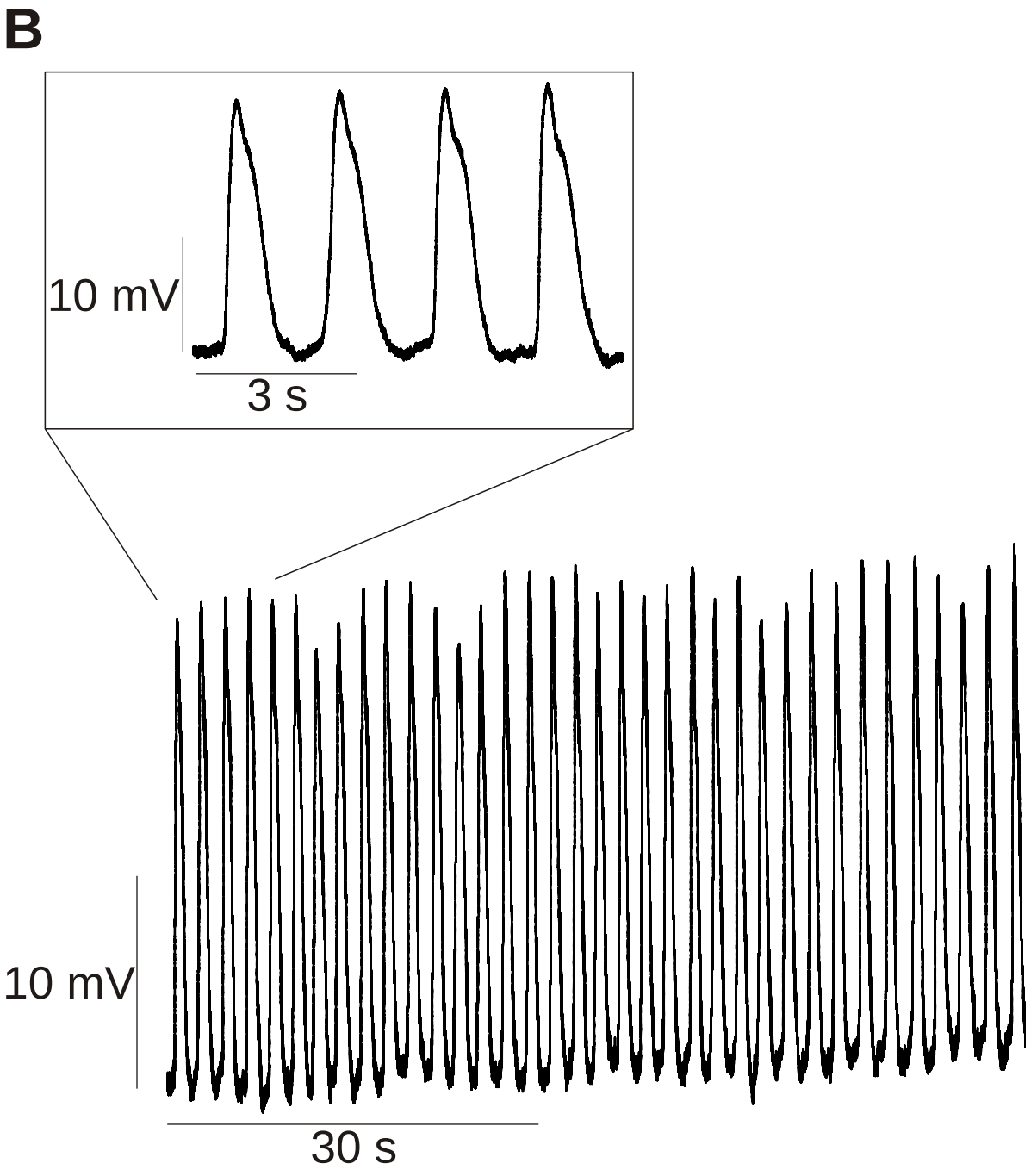
B
10 mV
3 s
10 mV
30 s

Table 4.1: Effects of *B. longum* supernatant, carbachol, and nitroarginine on the slow wave characteristics of the mouse jejunum

	MP							Waxing/Waning Pattern	
	Resting Membrane Potential (mV)	Frequency (cycles/ min.)	Upstroke Amplitude (mV)	Plateau Amplitude (mV)	Duration (s)	dV/dT Upstroke ($V\ s^{-1}$)	dV/dT Plateau ($V\ s^{-1}$)	Frequency (cycles/ min.)	Duration (s)
Krebs	-54.3 ± 7.4 (7)	26.0 ± 5.7 (7)	11.8 ± 5.5 (7)	11.3 ± 4.2 (7)	2.5 ± 0.9 (7)	.04 ± .03 (7)	.007 (1)	2.4 ± 5.2 (5)	2.4 ± 5.2 (5)
B.longum	-70.3 ± 13.9 (7)*****	24.1 ± 5.2 (7)	12.2 ± 4.7 (7)	12.6 ± 3.9 (7)	2.6 ± 0.7 (7)	.04 ± .03 (7)	.02 ± 0.0 (2)	--	--
Krebs	-58.8 ± 9.8 (6)	26.1 ± 7.0 (6)	13.2 ± 5.8 (6)	12.4 ± 5.0 (6)	2.4 ± 0.7 (6)	0.08 ± 0.1 (6)	--	2.6 (1)	2.6 (1)
LNNA ($2e^{-4}$M)	-54.3 ± 8.4 (6)	26.6 ± 7.5 (6)	15.4 ± 6.7 (6)	13.6 ± 4.2 (6)	2.4 ± 0.6 (6)	.08 ±.09 (6)	.03 (1)	2.2 ± 10.3 (5)	2.2 ± 10.3 (5)
Krebs	-58.1 ± 7.5 (7)	24.1 ± 4.1 (7)	10.1 ± 4.0 (7)	10.5 ± 4.6 (7)	2.4 ± 0.4 (7)	0.03 ± 0.4 (7)	0.02 (1)	2.6 (1)	2.6 (1)
CCh (1μM)	-47.7 ± 8.8 (7)*****	24.0 ± 5.7 (7)	10.5 ± 6.1 (7)	11.1 ± 6.6 (7)	2.5 ± 0.8 (7)	0.05 ± 0.07 (7)	0.03 (7)	2.4 ± 8.4 (4)	2.4 ± 8.4 (4)
Krebs alone	-52.9 ± 13.5 (14)	24.0 ± 5.6 (14)	12.4 ± 4.6 (14)	12.5 ± 4.8 (14)	2.6 ± 0.8 (14)	.04 ± .03 (14)	0.02 ± 0.01 (2)	2.0 ± 6.8 (4)	2.0 ± 6.8 (4)

Data is expressed as a mean ± S.D., with the numbers of observations in brackets.

4.4 Discussion

The effect of the perfusion of the conditioned medium on the circular smooth muscle of the jejunum of the mouse was an initial depolarization. During this depolarization, the amplitudes of the slow wave of these cells reduced until the slow wave completely disappeared and membrane potential began to plateau. A couple minutes after this plateau, the cells hyperpolarized and amplitudes as well as other slow wave characteristics returned to baseline levels similar to those prior to the addition of the conditioned medium. The resting membrane

potentials of these cells remained hyperpolarized thereafter. Occasionally, the cells would either solely depolarize or hyperpolarize upon the administration of the conditioned medium. Of course, in a physiological setting the depolarization of smooth muscle cells can be accompanied by a contraction of the muscle if the threshold of the L-type calcium channel is reached (Malysz et al., 1995) and hyperpolarization would lead to the opposite and relax the muscle. Although this multifaceted effect is peculiar, it is plausible by the simple fact that a supernatant is saturated with different substances that can act in different ways; some might have fast acting, transient effects while others display lengthier onset times with enduring effects. For example, the initial depolarization could be due to small molecules in the supernatant that can easily diffuse to the inside of the muscle cell, whereas the hyperpolarization could be from molecules in the supernatant that evoke a cascade event in the cell, and thus, take longer to manifest into an effect. It has been shown that products of bacterial metabolism in the human gut severely impact the metabolites produced in the host. Specifically, some indole-containing molecules arise only in the presence of a diverse microflora (Wikoff et al., 2009). The fact that the waxing and waning of the slow wave is abolished after the addition of the conditioned medium is very interesting. This waxing and waning pattern has been illustrated in the horse, cat, and mouse species; the origins of which are unresolved (Chang et al., 2001; Der-Silaphet, Malysz, Hagel, Arsenault, & Huizinga, 1998a; Diamant & Bortoff, 1969; Hudson et al., 2001; Huizinga, Ambrous, & Der-Silaphet, 1998a). When considering the results from the perfusion of the conditioned medium over AH cells, if the conditioned medium is also able to increase potassium conductance in enteric motor neurons then this would suggest that the waxing and waning of the slow wave is

stimulus dependent and possibly mediated through enteric nerves. It is important to keep in mind that in a physiological setting, *Bifidobacterium longum* NCC3001 would have to compete with other bacteria and therefore would not be able to proliferate to the colonies that they do when cultured. When bacterial cells are cultured, they are allowed to feed on nutrient rich media and can exponentially grow in numbers. When there is no competitive stress and the population is at its highest, these bacteria could produce complex polymers required to sustain a population at its plateau. In the gut, competition from other bacteria might not permit such synthesis of molecules and thus the effects observed in this *in situ* experiment may not reflect those in a physiological setting.

The results from the carbachol and L-NNA experiments were intriguing because upon the addition of either of these chemicals, the waxing and waning of the slow wave appeared when it was previously nonexistent. These results suggest that the trigger of the waxing and waning of the slow wave in circular smooth muscles is neuronal in origin. The interstitial cells of Cajal from the myenteric plexus (ICC-MP) are the pacemaker cells of the gastrointestinal tract (Huizinga et al., 1995) and generate a pacemaker potential that electrotonically spreads to neighbouring smooth muscle, where it is referred to as the slow wave (Kito & Suzuki, 2003). Our results suggest that perhaps the generation of the waxing and waning of the slow wave is mediated by the action of enteric neurons on interstitial cells of Cajal at the level of the myenteric plexus and possibly at the level of the deep muscular plexus. Intracellular microelectrode recordings from the circular smooth muscle at the level of the deep muscular plexus always revealed a slow wave associated with the ICC-MP and our results imply that

neuronal input is responsible for initiating this secondary pattern (waxing and waning) in either the ICC-MP themselves or interstitial cells of Cajal from the deep muscular plexus (ICC-DMP). It is particularly interesting if the waxing and waning is caused by the action of enteric neurons on the activity of ICC-DMP since it is already established that ICC-DMP play an important role in the neurotransmission of circular smooth muscle (X. Y. Wang, Sanders, & Ward, 1999; X. Y. Wang et al., 2003; Ward et al., 2006).

CHAPTER 5.0: GENERAL DISCUSSION

5.1 Summary of the major findings of the thesis

The overall objective of this thesis was two fold; the first was to determine if the supernatant from *Bifidobacterium longum* NCC3001 would have an effect on the excitability (electro-responsiveness) of AH cells as measured through spike discharge. The second objective was to determine the effects of the supernatant on the slow wave activity of the small intestine. In chapter 3.0, I showed that the supernatant can reduce a cell's excitability as measured through spike discharge, its input resistance, the magnitude of a hyperpolarization activated cationic current, and a reduction in the half width at half amplitude of their action potentials. A reduction in input resistance is indicative of increased potassium conductance and this increase is associated with cell hyperpolarization, which drives the cell further away from a depolarized state and an ability to fire an action potential. The hyperpolarization activated cationic current is a time-dependent sag in the voltage response of the cell to a hyperpolarizing current injection, which causes a depolarization of the cell. A reduction in the magnitude of the hyperpolarization activated cationic current means that the cell is relatively less depolarized and therefore further

away from the threshold of action potential generation. Lastly, we observed a reduction in the action potential half width duration. The fact that we observed this reduction in action potential duration at half width and as well a reduction in spike discharge and an increased potassium conductance after addition of the supernatant to an AH cell further confirms the premise that perhaps potassium channels are being opened. These findings suggest an inhibitory effect of the supernatant on the AH cell.

In chapter 4.0, I showed that the supernatant exhibited a multifaceted effect on the circular smooth muscle of the gut, causing an initial depolarization and a termination of slow waves and accompanied by a membrane potential plateau. Shortly after this plateau a hyperpolarization of the cell occurs and slow waves returned and remained. The frequency of the slow wave was unchanged throughout this multifaceted effect; however, the cell was significantly hyperpolarized approximately after two minutes of full immersion by the supernatant after the initial depolarization phase. Approximately half of all cells recorded from exhibited a waxing and waning of the slow wave and administration of the supernatant always abolished this pattern. Our results from the carbachol and nitroarginine treatment illustrated that by mimicking neurotransmission in the gut, we can induce the waxing and waning of the slow wave, suggesting a role of enteric motor neurons in the initiation of this pattern.

5.2 Reflections on the study

By studying the effect of the supernatant from *Bifidobacterium longum* NCC3001 on myenteric sensory neurons and potentially gut musculature, we gain insight into its mechanisms of action and the possible influences it has on motility. It is known that the enteric nervous

system communicates with the central nervous system (CNS) via the vagus in a manner that allows the CNS to monitor the state of the visceral organs. Also, it has been established that myenteric sensory neurons interact and form reflexes with other neurons in the gut wall that can cause changes in motility. Because sensory neurons of the enteric nervous system monitor the physical and chemical states of the gut lumen, it is conceivable to assume that the metabolites of *Bifidobacterium longum* NCC3001 can influence and possibly alter motility. Excitation of these neurons means depolarization and action potential generation when the threshold is reached and action potentials are a means of communication between neurons. These intrinsic (within gut wall) nerves eventually communicate with the extrinsic nerves and prevertebral ganglia, which eventually communicate with the CNS. For the above reasons, studying the effects of probiotics on neurons and musculature is critical in our understanding of the various patterns of motility that allow us to digest, absorb, and excrete foods.

Due to the nature of intracellular electrode recording, it was very difficult to maintain impalement in a neuron for extensive periods of time. This could be partly due to instabilities in the nitrogen vibration-free table, which if not working correctly can allow vibrations from the surrounding environment to reach the tip of the electrode, causing it to lose the impalement or damage the cell that is impaled in. Also, AH neurons are very sensitive with respect to their ability to fire. For example, if the cell transiently experiences a high intracellular calcium concentration, this can activate IK_{ca} channels that will allow potassium to leave the cell and cause hyperpolarization. If an AH neuron is too hyperpolarized, it will not reach threshold of activation of action potential generation and thus will be in a refractory period where it does not

fire. This scenario could be induced, for example, if the electrode vibrates or if there is a small perforation in the lipid bilayer, allowing calcium from the extracellular Krebs solution to enter the cell and cause hyperpolarization as described above. This is an example of why it is important to have large sample populations in a study of this nature so that any effect(s) observed by the supernatant are real effects and not due to the mechanical errors of the day-to-day experimentation. Furthermore, the longitudinal muscle-myenteric plexus (LMMP) preparation is effective in allowing the exposure of myenteric neurons; however, these conditions are far from the normal physiological circumstances. In this context, any data that are revealed using this preparation has to be further tested by other means to validate them in a physiological scenario.

Factors that are critical to obtaining accurate results and maintaining the viability of cells include: continuous and constant oxygenation of the solutions used to perfuse or immerse the tissue preparations in, practicing to minimize tears and holes in the LMMP preparations, and to not get in a habit of over-stimulating the neurons when trying to record membrane potential changes. Oxygenation is important because the cells in all mammalian tissue require constant oxygen in order to metabolize and stay lively and healthy. Minimizing the tears and perturbations to the LMMP preparation maintains the integrities of all networks (muscle, interstitial cells of cajal, and neurons), which increase the chances of recording from a cell by assuring that fewer cell are damaged. Furthermore, immersing the silver wire in bleach (sodium hypochlorite solution) or in other words ‘chloriding’ the silver wire electrode is very important in reducing noise from the electrodes and obtaining clean (*i.e.,* noise-free). This can be accomplished by placing the silver wires into bleach (sodium hypochlorite solution) for a

minimum period of 30 minutes. One can tell that the electrodes are adequately chlorided by the colour of the electrodes; a properly chlorided electrode will be black in colour, which is indicative of a good coating of silver chloride over the silver wire. A properly chlorided electrode permits the smooth transition of a flow of electrons from the wire to a flow of ions in the aqueous solution during recording.

5.3 Topics for further research

An important topic to address is the concentration factor of the supernatant dilution used in this thesis. Moreover, it would be particularly interesting to conduct the same experiments as in this thesis using different concentrations of supernatant to see whether the effects are more or less robust depending on the final concentration of the dilution. Perhaps, a more concentrated supernatant would yield a stronger effect and vice versa. Following the same principles, we can heat treat the supernatant to denature all proteins in the sample and check whether or not the effects previously described remain. Also, these experiments were conducted using an *in situ* preparation and it would be interesting to test the effects of *Bifidobacterium longum* NCC3001 on whole organ tissue. For example, we could test the effects of this bacterium on a cannulated jejunal segment of the small intestine in an organ bath to test the effects on circular muscle contraction and patterns of motility using spatio-temporal maps. Also, it would be interesting to test the effects of this probiotic on circular muscle strips in an organ bath with force transducers attached to either end of the muscle strip to test whether the muscle contracts or relaxes in the presence of the supernatant, or both. Together, these tools can help to elucidate the physiological effects of the supernatant of this bacterium on the small intestine of the mouse.

CHAPTER 6.0: REFERENCES

References

Abrams, G. D., & Bishop, J. E. (1967). Effect of the normal microbial flora on gastrointestinal motility. *Experimental Biology and Medicine, 126*(1), 301.

Antunes, L. C. M., Davies, J. E., & Finlay, B. B. (2011). Chemical signaling in the gastrointestinal tract. *F1000 Biology Reports, 3*

Bartho, L., Benko, R., Lazar, Z., Illenyi, L., & Horváth, Ö. (2002). Nitric oxide is involved in the relaxant effect of capsaicin in the human sigmoid colon circular muscle. *Naunyn-Schmiedeberg's Archives of Pharmacology, 366*(5), 496-500.

Bercik, P., Verdu, E. F., Foster, J. A., Macri, J., Potter, M., Huang, X., et al. (2010). Chronic gastrointestinal inflammation induces anxiety-like behavior and alters central nervous system biochemistry in mice. *Gastroenterology,*

Bertrand, P. P., Kunze, W. A., Bornstein, J. C., Furness, J. B., & Smith, M. L. (1997). Analysis of the responses of myenteric neurons in the small intestine to chemical stimulation of the mucosa. *American Journal of Physiology-Gastrointestinal and Liver Physiology, 273*(2), G422.

Bertrand, P. P., Kunze, W. A. A., Furness, J. B., & Bornstein, J. C. (2000). The terminals of myenteric intrinsic primary afferent neurons of the guinea-pig ileum are excited by 5-

hydroxytryptamine acting at 5-hydroxytryptamine-3 receptors. *Neuroscience, 101*(2), 459-469.

Caenepeel, P. H., Janssens, J., Vantrappen, G., Eyssen, H., & Coremans, G. (1989). Interdigestive myoelectric complex in germ-free rats. *Digestive Diseases and Sciences, 34*(8), 1180-1184.

Chang, I. Y., Glasgow, N. J., Takayama, I., Horiguchi, K., Sanders, K. M., & Ward, S. M. (2001). Loss of interstitial cells of cajal and development of electrical dysfunction in murine small bowel obstruction. *The Journal of Physiology, 536*(2), 555-568.

Chen, J. D. Z., Schirmer, B. D., & McCallum, R. W. (1993). Measurement of electrical activity of the human small intestine using surface electrodes. *Biomedical Engineering, IEEE Transactions on, 40*(6), 598-602.

Clerc, N., Furness, J. B., Bornstein, J. C., & Kunze, W. A. A. (1997). Correlation of electrophysiological and morphological characteristics of myenteric neurons of the duodenum in the guinea-pig. *Neuroscience, 82*(3), 899-914.

Clerc, N., Furness, J. B., Kunze, W. A. A., Thomas, E. A., & Bertrand, P. P. (1999). Long-term effects of synaptic activation at low frequency on excitability of myenteric AH neurons. *Neuroscience, 90*(1), 279-289.

Daniel, E. E., Wang, Y. F., & Cayabyab, F. S. (1998). Role of gap junctions in structural arrangements of interstitial cells of cajal and canine ileal smooth muscle. *American Journal of Physiology-Gastrointestinal and Liver Physiology, 274*(6), G1125-G1141.

Der-Silaphet, T., Malysz, J., Hagel, S., Arsenault, A. L., & Huizinga, J. D. (1998a). Interstitial cells of cajal direct normal propulsive contractile activity in the mouse small intestine. *Gastroenterology, 114*(4), 724-736.

Der-Silaphet, T., Malysz, J., Hagel, S., Arsenault, A. L., & Huizinga, J. D. (1998b). Interstitial cells of cajal direct normal propulsive contractile activity in the mouse small intestine. *Gastroenterology, 114*(4), 724-736.

Diamant, N. E., & Bortoff, A. (1969). Nature of the intestinal low-wave frequency gradient. *American Journal of Physiology--Legacy Content, 216*(2), 301.

Donnelly, G., Jackson, T. D., Ambrous, K., Ye, J., Safdar, A., Farraway, L., et al. (2001). The myogenic component in distention-induced peristalsis in the guinea pig small intestine. *American Journal of Physiology-Gastrointestinal and Liver Physiology, 280*(3), G491-G500.

Ferens, D., Baell, J., Lessene, G., Smith, J. E., & Furness, J. B. (2007). Effects of modulators of Ca2 ‐activated, intermediate ‐conductance potassium channels on motility of the rat small intestine, in vivo. *Neurogastroenterology & Motility, 19*(5), 383-389.

Fioramonti, J., Theodorou, V., & Bueno, L. (2003). Probiotics: What are they? what are their effects on gut physiology? *Best Practice & Research Clinical Gastroenterology, 17*(5), 711-724.

Furness, J. B. (2006). *The enteric nervous system* Wiley-Blackwell.

Furness, J. B., Alex, G., Clark, M. J., & Lal, V. V. (2003). Morphologies and projections of defined classes of neurons in the submucosa of the guinea‐pig small intestine. *The Anatomical Record Part A: Discoveries in Molecular, Cellular, and Evolutionary Biology, 272*(2), 475-483.

Furness, J. B., Kearney, K., Robbins, H. L., Hunne, B., Selmer, I. S., Neylon, C. B., et al. (2004). Intermediate conductance potassium (IK) channels occur in human enteric neurons. *Autonomic Neuroscience, 112*(1-2), 93-97.

Hillsley, K., Kenyon, J. L., & Smith, T. K. (2000). Ryanodine-sensitive stores regulate the excitability of AH neurons in the myenteric plexus of guinea-pig ileum. *Journal of Neurophysiology, 84*(6), 2777.

Hirst, G. D. S., Holman, M. E., & Spence, I. (1974). Two types of neurones in the myenteric plexus of duodenum in the guinea-pig. *The Journal of Physiology, 236*(2), 303-326.

Holaday, D. A., Volk, H., & Mandell, J. (1958). Electrical activity of the small intestine with special reference to the origin of rhythmicity. *American Journal of Physiology--Legacy Content, 195*(2), 505.

Hudson, N. P. H., Mayhew, I. G., & Pearson, G. T. (2001). In vitro microelectrode study of the electrical properties of smooth muscle in equine ileum. *Veterinary Record, 149*(23), 707.

Huizinga, J. D., Ambrous, K., & Der-Silaphet, T. (1998a). Co-operation between neural and myogenic mechanisms in the control of distension-induced peristalsis in the mouse small intestine. *The Journal of Physiology, 506*(3), 843.

Huizinga, J. D., Ambrous, K., & Der-Silaphet, T. (1998b). Co-operation between neural and myogenic mechanisms in the control of distension-induced peristalsis in the mouse small intestine. *The Journal of Physiology, 506*(3), 843.

Huizinga, J. D., Thuneberg, L., Kluppel, M., Malysz, J., Mikkelsen, H. B., & Bernstein, A. (1995). W/kit gene required for interstitial cells of cajal and for intestinal pacemaker activity. *Nature, 373*(6512), 347-349.

Kamiya, T., Wang, L., Forsythe, P., Goettsche, G., Mao, Y., Wang, Y., et al. (2006). Inhibitory effects of lactobacillus reuteri on visceral pain induced by colorectal distension in sprague-dawley rats. *Gut, 55*(2), 191.

Kidd, M., Gustafsson, B., Drozdov, I., & Modlin, I. (2009). IL1β‐and LPS‐induced serotonin secretion is increased in EC cells derived from Crohn's disease. *Neurogastroenterology & Motility, 21*(4), 439-450.

Kirchgessner, A. L., Liu, M. T., & Gershon, M. D. (1996). In situ identification and visualization of neurons that mediate enteric and enteropancreatic reflexes. *The Journal of Comparative Neurology, 371*(2), 270-286.

Kirchgessner, A., Tamir, H., & Gershon, M. (1992). Identification and stimulation by serotonin of intrinsic sensory neurons of the submucosal plexus of the guinea pig gut: Activity-induced expression of fos immunoreactivity. *The Journal of Neuroscience, 12*(1), 235-248.

Kito, Y., & Suzuki, H. (2003). Properties of pacemaker potentials recorded from myenteric interstitial cells of cajal distributed in the mouse small intestine. *The Journal of Physiology, 553*(3), 803-818.

Kito, Y., Ward, S. M., & Sanders, K. M. (2005). Pacemaker potentials generated by interstitial cells of cajal in the murine intestine. *American Journal of Physiology-Cell Physiology, 288*(3), C710-C720.

Kunze, W. A., Mao, Y. K., Wang, B., Huizinga, J. D., Ma, X., Forsythe, P., et al. (2009). Lactobacillus reuteri enhances excitability of colonic AH neurons by inhibiting calcium‐

dependent potassium channel opening. *Journal of Cellular and Molecular Medicine, 13*(8b), 2261-2270.

Kunze, W. A. A., Bornstein, J. C., & Furness, J. B. (1995). Identification of sensory nerve cells in a peripheral organ (the intestine) of a mammal. *Neuroscience, 66*(1), 1-4.

Kunze, W. A. A., Clerc, N., Bertrand, P. P., & Furness, J. B. (1999). Contractile activity in intestinal muscle evokes action potential discharge in guinea‐pig myenteric neurons. *The Journal of Physiology, 517*(2), 547-561.

Kunze, W. A. A., Clerc, N., Furness, J. B., & Gola, M. (2000). The soma and neurites of primary afferent neurons in the guinea‐pig intestine respond differentially to deformation. *The Journal of Physiology, 526*(2), 375-385.

Kunze, W. A. A., & Furness, J. B. (1999). The enteric nervous system and regulation of intestinal motility. *Annual Review of Physiology, 61*(1), 117-142.

Kunze, W. A. A., Furness, J. B., Bertrand, P. P., & Bornstein, J. C. (1998). Intracellular recording from myenteric neurons of the guinea-pig ileum that respond to stretch. *The Journal of Physiology, 506*(3), 827-842.

Kunze, W. A. A., Furness, J. B., & Bornstein, J. C. (1993). Simultaneous intracellular recordings from enteric neurons reveal that myenteric AH neurons transmit via slow excitatory postsynaptic potentials. *Neuroscience, 55*(3), 685-694.

Li, Y., Hao, Y., Zhu, J., & Owyang, C. (2000). Serotonin released from intestinal enterochromaffin cells mediates luminal non-cholecystokinin-stimulated pancreatic secretion in rats. *Gastroenterology, 118*(6), 1197-1207.

Li, Z. S., & Furness, J. B. (2000). Inputs from intrinsic primary afferent neurons to nitric oxide synthase-immunoreactive neurons in the myenteric plexus of guinea pig ileum. *Cell and Tissue Research, 299*(1), 1-8.

Lowie, B. J., Wang, X. Y., White, E. J., & Huizinga, J. D. (2011). On the origin of rhythmic calcium transients in the ICC-MP of the mouse small intestine. *American Journal of Physiology-Gastrointestinal and Liver Physiology, 301*(5), G835-G845.

Ma, X., Mao, Y. K., Wang, B., Huizinga, J. D., Bienenstock, J., & Kunze, W. (2009). Lactobacillus reuteri ingestion prevents hyperexcitability of colonic DRG neurons induced by noxious stimuli. *American Journal of Physiology-Gastrointestinal and Liver Physiology, 296*(4), G868.

Malysz, J., Richardsons, D., Farraway, L., Huizinga, J. D., & Christen, M. O. (1995). Generation of slow wave type action potentials in the mouse small intestine involves a non-L-type calcium channel. *Canadian Journal of Physiology and Pharmacology, 73*(10), 1502-1511.

Mao, Y., Wang, B., & Kunze, W. (2006). Characterization of myenteric sensory neurons in the mouse small intestine. *Journal of Neurophysiology, 96*(3), 998-1010.

Nakagawa, T., Misawa, H., Nakajima, Y., & Takaki, M. (2005). Absence of peristalsis in the ileum of W/W v mutant mice that are selectively deficient in myenteric interstitial cells of cajal. *Journal of Smooth Muscle Research, 41*(3), 141-151.

Park, K. J., Hennig, G. W., Lee, H. T., Spencer, N. J., Ward, S. M., Smith, T. K., et al. (2006). Spatial and temporal mapping of pacemaker activity in interstitial cells of cajal in mouse ileum in situ. *American Journal of Physiology-Cell Physiology, 290*(5), C1411.

Pompolo, S., & Furness, J. B. (1988). Ultrastructure and synaptic relationships of calbindin-reactive, dogiel type II neurons, in myenteric ganglia of guinea-pig small intestine. *Journal of Neurocytology, 17*(6), 771-782.

Powley, T. L., & Phillips, R. J. (2011). Vagal intramuscular array afferents form complexes with interstitial cells of cajal in gastrointestinal smooth muscle: Analogues of muscle spindle organs? *Neuroscience,*

Racke, K., Reimann, A., Schwörer, H., & Kilbinger, H. (1995). Regulation of 5-HT release from enterochromaffin cells. *Behavioural Brain Research, 73*(1-2), 83-87.

Rugiero, F., Gola, M., Kunze, W. A. A., Reynaud, J. C., Furness, J. B., & Clerc, N. (2002). Analysis of whole‐cell currents by patch clamp of guinea‐pig myenteric neurones in intact ganglia. *The Journal of Physiology, 538*(2), 447-463.

Rumessen, J. J., Mikkelsen, H. B., & Thuneberg, L. (1992). Ultrastructure of interstitial cells of cajal associated with deep muscular plexus of human small intestine. *Gastroenterology, 102*(1), 56.

Stagg, A., Hart, A., Knight, S., & Kamm, M. (2003). The dendritic cell: Its role in intestinal inflammation and relationship with gut bacteria. *Gut, 52*(10), 1522.

Suzuki, N., Prosser, C. L., & Dahms, V. (1986). Boundary cells between longitudinal and circular layers: Essential for electrical slow waves in cat intestine. *American Journal of Physiology-Gastrointestinal and Liver Physiology*, *250*(3), G287-G294.

Torihashi, S., Fujimoto, T., Trost, C., & Nakayama, S. (2002). Calcium oscillation linked to pacemaking of interstitial cells of cajal. *Journal of Biological Chemistry, 277*(21), 19191-19197.

Vanden Berghe, P., Kenyon, J. L., & Smith, T. K. (2002). Mitochondrial Ca2 uptake regulates the excitability of myenteric neurons. *The Journal of Neuroscience, 22*(16), 6962.

Verdú, E. F., Bercík, P., Bergonzelli, G. E., Huang, X. X., Blennerhasset, P., Rochat, F., et al. (2004). Lactobacillus paracasei normalizes muscle hypercontractility in a murine model of postinfective gut dysfunction. *Gastroenterology*, *127*(3), 826-837.

Verdu, E. F., Bercik, P., Verma-Gandhu, M., Huang, X. X., Blennerhassett, P., Jackson, W., et al. (2006). Specific probiotic therapy attenuates antibiotic induced visceral hypersensitivity in mice. *Gut, 55*(2), 182.

Wang, B., Mao, Y., Diorio, C., Wang, L., Huizinga, J. D., Bienenstock, J., et al. (2010a). Lactobacillus reuteri ingestion and IKCa channel blockade have similar effects on rat colon motility and myenteric neurones. *Neurogastroenterology & Motility, 22*(1), 98-e33.

Wang, B., Mao, Y., Diorio, C., Wang, L., Huizinga, J., Bienenstock, J., et al. (2010b). Lactobacillus reuteri ingestion and IKCa channel blockade have similar effects on rat colon motility and myenteric neurones. *Neurogastroenterology & Motility, 22*(1), 98-e33.

Wang, B., Mao, Y. K., Diorio, C., Pasyk, M., Wu, R. Y., Bienenstock, J., et al. (2010). Luminal administration ex vivo of a live lactobacillus species moderates mouse jejunal motility within minutes. *The FASEB Journal, 24*(10), 4078-88.

Wang, X. Y., Paterson, C., & Huizinga, J. D. (2003). Cholinergic and nitrergic innervation of ICC‐DMP and ICC‐IM in the human small intestine. *Neurogastroenterology & Motility, 15*(5), 531-543.

Wang, X. Y., Sanders, K. M., & Ward, S. M. (1999). Intimate relationship between interstitial cells of cajal and enteric nerves in the guinea-pig small intestine. *Cell and Tissue Research, 295*(2), 247-256.

Wang, X. Y., Vannucchi, M. G., Nieuwmeyer, F., Ye, J., Faussone-Pellegrini, M. S., & Huizinga, J. D. (2005). Changes in interstitial cells of cajal at the deep muscular plexus are associated with loss of distention-induced burst-type muscle activity in mice infected by trichinella spiralis. *The American Journal of Pathology, 167*(2), 437.

Ward, S. M., McLaren, G. J., & Sanders, K. M. (2006). Interstitial cells of cajal in the deep muscular plexus mediate enteric motor neurotransmission in the mouse small intestine. *The Journal of Physiology, 573*(1), 147-159.

Wikoff, W. R., Anfora, A. T., Liu, J., Schultz, P. G., Lesley, S. A., Peters, E. C., et al. (2009). Metabolomics analysis reveals large effects of gut microflora on mammalian blood metabolites. *Proceedings of the National Academy of Sciences, 106*(10), 3698.

Wood, J. D., & Mayer, C. J. (1978). Slow synaptic excitation mediated by serotonin in auerbach's plexus.*276*, 836-837.

Yamazawa, T., & Iino, M. (2002). Simultaneous imaging of Ca2 signals in interstitial cells of cajal and longitudinal smooth muscle cells during rhythmic activity in mouse ileum. *The Journal of Physiology, 538*(3), 823.

CHAPTER 7.0: APPENDICES

7.1 List of Publications

P. Bercik, P., Park, A.J., Sinclair, D., Khoshdel, A., Lu, J., Huang, X., Deng, Y., Blennerhassett, P.A., Fahnestock, M., Moine, D., Berger, B., Huizinga, J., Kunze, W., McLean, P.G., Bergonzelli, G.E., Collins, S.M., Verdu, E.F. (2011) The anxiolytic effect of *Bifidobacterium longum* NCC3001 involves vagal pathways for gut–brain communication. *Neurogastroenterol. Motil.* 23 (12): 1132-1139.